


Classical and quantum thermodynamics in a non-equilibrium regime: Application to Stirling engine

Shoki Koyanagi ^{a)} and Yoshitaka Tanimura ^{a)}

Department of Chemistry, Graduate School of Science, Kyoto University, Kyoto 606-8502, Japan

(Dated: Last updated: 29 May 2024)

We develop a thermodynamic theory in the non-equilibrium regime by extending a theory based on the dimensionless (DL) minimum work principle previously developed for a thermodynamic system-bath model [S. Koyanagi and Y. Tanimura, J. Chem. Phys. in press (<http://arxiv.org/abs/2405.16787>)]. Our results are described by non-equilibrium thermodynamic potentials expressed in time-derivative form in terms of extensive and intensive variables. This is made possible through the incorporation of waste heat, which is equivalent to the loss work consumed by the bath, into the definitions of thermodynamic potentials in a non-equilibrium regime. These potentials can be evaluated from the DL non-equilibrium-to-equilibrium minimum work principle, which is derived from the principle of DL minimum work and is equivalent to the second law of thermodynamics. We thus obtain the non-equilibrium Massieu-Planck potentials as entropic potentials and the non-equilibrium Helmholtz-Gibbs potentials as free energies. Our results are verified numerically by simulating a Stirling engine consisting of two isothermal and two thermostatic processes using the quantum Fokker-Planck equations and the classical Kramers equation derived from the thermodynamic system-bath model. We then show that any thermodynamic process can be analyzed using a non-equilibrium work diagram analogous to the equilibrium one for given time-dependent intensive variables. The results can be used to develop efficient heat machines in non-equilibrium regimes.

I. INTRODUCTION

Ever since Carnot explored the efficiency of heat engines 200 years ago,¹ there have been longstanding attempts to study thermodynamics in non-equilibrium regimes, driven by both academic curiosity and practical interest. In particular, recent advances in nanotechnology have led to increased interest in the study of the thermodynamics of microscopic quantum systems.^{2–22}

As a kinetic theory, such phenomena are typically explained using open quantum dynamics theories based on the system-bath (SB) model.^{23–26} Although thermodynamics is a system-independent theory, it is derived from the presence of a heat bath and is consistent with theories based on the SB model.¹⁷ The main (subsystem) system of the SB model can describe a variety of systems, from a simple two-level system to complex molecular systems with many degrees of freedom, and it is also possible to take the classical limit in the case where the system can be described in phase space.^{24–31} Under the condition of a heat bath with infinite degrees of freedom, the total system irreversibly relaxes toward its equilibrium state in time, and so the second law of thermodynamics is naturally obeyed without the need for the assumption of ergodicity as a dynamical system.^{29–32}

However, to investigate whether the thermodynamic laws are satisfied even in quantum cases where the subsystem and bath are quantum mechanically entangled, it is necessary to treat the bath in a non-Markovian and

nonperturbative manner so that the thermal equilibrium state of the total systems satisfies the energy conservation law, including the SB interaction. Therefore, equations of motion derived using the Markovian or rotational wave (or secular) approximation, such as the Lindblad equation and the quantum master equation, can only be applied to high-temperature regions where the subsystem exhibits semiclassical dynamics.^{29–32} Over the past 30 years, several methodologies have been developed to accurately describe the effects of quantum entanglement for condensed systems while maintaining strict energy conservation to satisfy the first law of thermodynamics. Such methods include the hierarchical equations of motion (HEOM),^{27–33} the quasi-adiabatic path integral (QUAPI),^{34–40} and multiconfigurational time-dependent Hartree (MCTDH).^{41–43} Among these, the HEOM approach is ideal for thermodynamic investigations, not only because it can perform numerically “exact” dynamic simulations, but also because it can evaluate the change in energy of the heat bath and the SB interaction separately, even for processes far from equilibrium.^{20–22,44–51}

While the difficulty of numerical simulation has been solved, there is a fundamental difference between open quantum dynamics theory, which is based on a first-principles description of kinetic systems from a microscopic perspective, and thermodynamic theory, which is based on a phenomenological description of thermal systems from a macroscopic perspective. For example, in quantum mechanics, observables are defined as expectation values, whereas in thermodynamics, they are described by macroscopic intensive and extensive variables. Furthermore, quantum mechanics is a formalism for time evolution, whereas thermodynamics deals primarily with static and quasi-static states near thermal equilibrium. In

^{a)} Authors to whom correspondence should be addressed: koyanagi.syoki.36z@st.kyoto-u.jp and tanimura.yoshitaka.5w@kyoto-u.jp

this respect, most studies of quantum thermodynamics are merely kinetic simulations of open quantum dynamics, and their relation to thermodynamics has not been studied in depth. Thus, the fundamental difference between microscopic quantum mechanics and macroscopic thermodynamics raises many open questions, such as whether the Carnot limit can be violated in a quantum case or the existence of Maxwell's demon.

The virtue of thermodynamics lies in its ability to describe macroscopic thermal phenomena resulting from complex microscopic interactions in a system-independent manner as changes in thermodynamic potentials described as interrelated intensive and extensive variables through Legendre transformations. This virtue should be preserved when we develop a quantum thermodynamic theory rather than an open quantum dynamical theory, although in either case, the theory must be specific to the SB model.

It has been found that the Gibbs energy can be obtained directly from kinetic simulations or experiments based on the minimum work principle (or Kelvin–Planck statement), expressed as $W(t) \geq \Delta G(t)$, where $W(t)$ is the work done from the outside to the subsystem by external fields and $\Delta G(t)$ is the change in free energy, by evaluating the work in a quasi-static process,^{20,44} which allows us to draw a work diagram corresponding to the P – V diagram.^{49,50} However, with this approach, the contributions of temperature T and entropy S in the thermodynamic potential expressed as TdS and SdT cannot be evaluated, because the minimum work principle is defined as an isothermal process $dT = 0$.

To overcome this limitation, we developed a thermostatic SB model that is defined by a system coupled to multiple heat baths with different temperatures.⁵¹ We then extended the minimum work principle to thermostatic processes in a dimensionless (DL) form (the DL minimum work principle) as $\tilde{W}(t) \geq \Delta \Xi(t)$, where $\tilde{W}(t) \equiv \beta(t)W(t)$ is the DL (entropic) work, with $\beta(t) \equiv 1/k_B T(t)$ (where k_B is the Boltzmann constant) being the time-dependent inverse temperature, and $\Delta \Xi$ is the change in the DL Planck potential.⁵¹ Not only intensive variables but also extensive variables, which are related by the time-dependent Legendre transformations, were introduced as quantum expectation values of the SB system. The validity of these results has been numerically verified using the low-temperature quantum Fokker–Planck equations in the quantum case and the Kramers equation in the classical case,⁵² both developed for the thermodynamic SB model.⁵¹ Although these results were restricted to quasi-static cases, the definitions of the thermodynamic potentials, intensive and extensive variables, and Legendre transformations were defined in such a way that they hold for any non-equilibrium process. Taking advantage of this, we extend our thermodynamic theory here to the non-equilibrium regime.

The rest of this paper is organized as follows. In Sec. II, our previous results are summarized with regard to thermodynamics as applied to work in a system-independent

manner. We then derive the principle of non-equilibrium DL minimum work to obtain the DL Massieu–Planck potentials and Helmholtz–Gibbs potentials in the non-equilibrium regime. Results are verified in Sec. III by numerical simulations using the SB model. Finally, Sec. IV presents concluding remarks.

II. REFLECTIONS ON WORK OF HEAT

In our previous paper,⁵¹ we presented system-specific thermodynamic laws based on open quantum dynamics theory. Here, we develop the same laws by introducing several thermodynamic “statements” without going into the details of the system, as in traditional thermodynamic theory. By doing so, we clarify the distinctive features of thermodynamic theory that allow it to treat systems in non-equilibrium regimes.

A. Laws of thermodynamics as applied to work

We consider a thermodynamic system consisting of a subsystem A and a heat bath B at an inverse temperature $\beta(t)$. The presence of a heat bath temperature can be regarded as a consequence of **the zeroth law of thermodynamics**.

An important statement of thermodynamics is that thermodynamic systems are described in terms of intensive and extensive variables. In particular, extensive variables that are proportional to the size are essential. This statement, controversial, is sometimes called the fourth law.⁵³ However, this is the premise of thermodynamics and we should call **the minus first law of thermodynamics**.

The energy of the subsystem corresponds to internal energy and is expressed as $U_A(t)$, which changes with time owing to changes in the bath temperature. Internal energy is an extensive variable, whereas inverse temperature is an intensive variable. The external perturbation we consider here is expressed as $-x(t)X_A(t)$, where $x(t)$ and $X_A(t)$ are intensive and extensive variables, respectively. In traditional thermodynamics, $x(t)$ is derived from the Euler relation. We then introduce the total energy, which is related to enthalpy by $H_A(t) = U_A(t) - x(t)X_A(t)$, which can also be regarded as the Legendre transformation between internal energy and enthalpy.

Because $U_A(t)$ is the conjugate variable of $\beta(t)$, we introduce the DL (or entropic) internal energy denoted by $\tilde{U}_A(t)$, where $\tilde{B}(t) \equiv \beta(t)B(t)$ for any variable $B(t)$. Because $\beta(t)$ diverges for $T \rightarrow 0$, states with $T = 0$ do not exist, which corresponds to **the third law of thermodynamics**.

From the time derivative of the DL internal energy

$\tilde{U}_A(t)$, we have

$$\frac{d\tilde{U}_A(t)}{dt} = \frac{d\tilde{W}_A^{ext}(t)}{dt} + \frac{d\tilde{Q}_A^{ext}(t)}{dt}, \quad (1)$$

where

$$\frac{d\tilde{W}_A^{ext}(t)}{dt} = U_A(t) \frac{d\beta(t)}{dt} + \tilde{x}(t) \frac{dX_A(t)}{dt} \quad (2)$$

and

$$\frac{d\tilde{Q}_A^{ext}(t)}{dt} \equiv \beta(t) \frac{dU_A(t)}{dt} - \tilde{x}(t) \frac{dX_A(t)}{dt} \quad (3)$$

are the DL (or entropic) extensive work defined as being done from the outside and DL (or entropic) extensive heat, respectively. For the enthalpy, we have

$$\frac{d\tilde{H}_A(t)}{dt} = \frac{d\tilde{W}_A^{int}(t)}{dt} + \frac{d\tilde{Q}_A^{ext}(t)}{dt}, \quad (4)$$

where

$$\frac{d\tilde{W}_A^{int}(t)}{dt} \equiv U_A(t) \frac{d\beta(t)}{dt} - X_A(t) \frac{d\tilde{x}(t)}{dt} \quad (5)$$

is the intensive work. Equations (1) and (4) correspond to **the first law of thermodynamics**.

From the definitions, these intensive and extensive variables satisfy the time-dependent Legendre (TDL) transformation expressed as

$$\frac{d\tilde{W}_A^{int}(t)}{dt} = \frac{d\tilde{W}_A^{ext}(t)}{dt} - \frac{d}{dt} [\tilde{x}(t) X_A(t)]. \quad (6)$$

Equation (1) is also expressed in the form of the TDL transformation as

$$\frac{d\tilde{W}_A^{ext}(t)}{dt} = -\frac{d\tilde{Q}_A^{ext}(t)}{dt} + \frac{d}{dt} [\beta(t) U_A(t)]. \quad (7)$$

The intensive heat $\tilde{Q}_A^{int}(t)$ can also be defined from $\tilde{Q}_A^{ext}(t)$ using the TDL [Eq. (A2) in Appendix A]. While the above equations, including the first law of thermodynamics, hold for any non-equilibrium processes described by intensive variables $\beta(t)$ and $\tilde{x}(t)$ and extensive variables $U_A(t)$ and $X_A(t)$ which are the state variables, as they are kinematic observables at time t , work and heat are not state variables.

As **the second law of thermodynamics**, we adopt **the DL minimum work principle** for the subsystem from one equilibrium state to another, which extends the Kelvin-Planck statement for isothermal processes to thermostatic processes. For work defined as being done from the outside to the subsystem, we have

$$\tilde{W}_A^{ext} \geq -\Delta\Phi_A^{qst}, \quad (8)$$

where Φ_A^{qst} is the DL Massieu potential⁵⁴ and equality holds under quasi-static changes of natural variables $\beta(t)$ and $X_A(t)$ as $\Phi_A^{qst}[\beta^{qst}, X_A^{qst}] = \tilde{W}_A^{ext}[\beta^{qst}, X_A^{qst}]$. The

above inequality states that for any process occurring between two states, the work done from the outside is minimized if the process is quasistatic (or reversible), because no energy is dissipated in the heat bath. Note that if we define work as being done from the subsystem to outside, the inequality in Eq.(8) is reversed and the relationship is called the maximum work principle (to the outside). Using the TDL transformation (6), we also have the Planck potential⁵⁵ in terms of natural variables expressed as $\Xi_A^{qst}[\beta^{qst}, \tilde{x}^{qst}]$ (see Appendix A).

For the DL extensive heat $\tilde{Q}_A^{ext}(t)$, we have

$$\tilde{Q}_A^{ext} \leq \Delta\Lambda_A^{qst}, \quad (9)$$

which corresponds to **the principle of maximum entropy**, where $\Lambda_A^{qst}[U_A^{qst}, X_A^{qst}]$ is the entropic potential. Because both natural variables are extensive, this potential is fundamental and we call it Massieu entropy (M-entropy). Using the TDL transformation Eq. (A2), we also have Planck entropy (P-entropy) defined by $\Gamma_A^{qst}[U_A^{qst}, \tilde{x}^{qst}]$ from $\tilde{Q}_A^{int}(t)$ (see Appendix A). Similar to the entropy obtained from the partition function in statistical physics, this entropy is a function of the extensive variable \tilde{x}^{qst} .

Here, as the conjugate variable for $\beta(t)$, we chose the internal energy U_A^{qst} , which is considered a fundamental variable in thermodynamics, but enthalpy H_A^{qst} could also be chosen⁵¹. In such case, there are also two entropies, one involving both extensive variables (Clasius entropy or C-entropy) and one for intensive variable with respect to external forces (Boltzmann entropy or B-entropy). The B-entropy and M-entropy are related to the others by the Legendre transformations between U_A^{qst} and H_A^{qst} and the values do not change, although the former includes one intensive variable whereas the later includes extensive variables only. However, there is no explicit relationship between C-entropy and M-entropy, because the Legendre transformation between two entropy in the U_A^{qst} representation and the H_A^{qst} representation are different. (See Appendix D in Ref. 51). In any case, the Massieu-Planck potentials are entropic potentials.⁵⁶

The total differential form of the Helmholtz-Gibbs potentials can be derived from the Massieu-Planck potentials using the definitions $F_A^{qst}(t) = -\Phi_A^{qst}(t)/\beta^{qst}(t)$ and $G_A^{qst}(t) = -\Xi_A^{qst}(t)/\beta^{qst}(t)$. The results are summarized and presented in Table VI in Appendix A.

B. Thermodynamic potentials in a non-equilibrium regime

1. The DL non-equilibrium minimum work principle

On the basis of Eq. (8), we can define thermodynamic potentials applicable to the non-equilibrium regime. Consider a non-equilibrium state A and equilibrium state n . **The DL non-equilibrium-to-equilibrium minimum work principle** for $A \rightarrow n$ is expressed as (see

Appendix B)

$$(\tilde{W}_A^{ext})_{A \rightarrow n} \geq -(\Delta\Phi_A^{neq})_{A \rightarrow n}, \quad (10)$$

where $\Phi_A^{neq}(t)$ is the non-equilibrium Massieu potential. This inequality indicates that the path from non-equilibrium to equilibrium has a lower bound on work. In engineering, the effective energy from non-equilibrium to equilibrium is referred to as exergy.^{57,58} The non-equilibrium thermodynamic potential we introduced here can be regarded as a generalization of it.

The difference between $(\tilde{W}_A^{ext})_{A \rightarrow n}$ and $-(\Delta\Phi_A^{neq})_{A \rightarrow n}$ corresponds to the DL heat generated as loss work, denoted by $-(\tilde{Q}_A^{wst})_{A \rightarrow n}$, which we call DL waste heat:

$$-(\tilde{Q}_A^{wst})_{A \rightarrow n} = (\tilde{W}_A^{ext})_{A \rightarrow n} + (\Delta\Phi_A^{neq})_{A \rightarrow n} \geq 0. \quad (11)$$

Because the DL waste heat between two non-equilibrium states A and B is evaluated as $(\tilde{Q}_A^{wst})_{A \rightarrow B} = (\tilde{Q}_A^{wst})_{A \rightarrow n} - (\tilde{Q}_B^{wst})_{B \rightarrow n}$, we the waste heat for any non-equilibrium process at times t and $t + dt$ (where dt is an infinitesimal time) in time-derivative form:

$$-\frac{d\tilde{Q}_A^{wst}(t)}{dt} = \frac{d\tilde{W}_A^{ext}(t)}{dt} + \frac{d\Phi_A^{neq}(t)}{dt}. \quad (12)$$

As shown in Appendix B, the waste heat is nonpositive, i.e., $d\tilde{Q}_A^{wst}(t)/dt \leq 0$. Thus, we have the inequality $(\tilde{W}_A^{ext})_{A \rightarrow B}^{\min} \geq -(\Delta\Phi_A^{neq})_{A \rightarrow B}$, or

$$\frac{d\tilde{W}_A^{ext}(t)}{dt} \geq -\frac{d\Phi_A^{neq}(t)}{dt}, \quad (13)$$

which we call **the DL non-equilibrium minimum work principle**. While $\tilde{W}_A^{ext}(t)$ and $\tilde{Q}_A^{wst}(t)$ are not state variables because they depend on a path, $\Phi_A^{neq}(t)$ is a state variable defined by the non-equilibrium-to-equilibrium minimum work path. When state B is on the non-equilibrium-to-equilibrium minimum work path from A to n , equality holds in (13).

Using Eqs. (2) and (12), we obtain the time-derivative form of the non-equilibrium Massieu potential as

$$\frac{d\Phi_A^{neq}(t)}{dt} = -U_A^{neq} \frac{d\beta(t)}{dt} - \tilde{x}(t) \frac{dX_A^{neq}(t)}{dt} - \frac{d\tilde{Q}_A^{wst}(t)}{dt} \quad (14)$$

The convexity of DL potentials is discussed on the basis of the SB model in Appendix C. Thus, we can regard these as thermodynamic potentials.

Using Eqs. (6), we have the non-equilibrium Planck potential expressed as

$$\frac{d\Xi_A^{neq}(t)}{dt} = -U_A^{neq} \frac{d\beta(t)}{dt} + X_A^{neq}(t) \frac{d\tilde{x}(t)}{dt} - \frac{d\tilde{Q}_A^{wst}(t)}{dt} \quad (15)$$

The M-entropy $\Lambda_A^{neq}(t)$ and P-entropy $\Gamma_A^{neq}(t)$ can be evaluated from the TDL transformations (6) and (7). The non-equilibrium potentials satisfy the Legendre transformations:

$$\Xi_A^{neq}(t) = \Phi_A^{neq}(t) + \tilde{x}(t)X_A^{neq}(t) \quad (16)$$

and

$$\Lambda_A^{neq}(t) = \Phi_A^{neq}(t) + \beta(t)U_A^{neq}(t). \quad (17)$$

The time-derivative forms of the DL non-equilibrium entropic potentials are summarized in Table I. Note that while the entropic potentials, the intensive variables and non-equilibrium extensive variables are state variables, the time-derivative of them including waste heat are not state variables.

As shown in Appendix D, the non-equilibrium Massieu potential is always smaller than the quasi-static Massieu potential. This indicates that the non-equilibrium Massieu potential is minimum when the state is equilibrium. In the quasi-static case, Table I is reduced to Table V (Appendix A). Thus, we can regard these potentials as extensions of the thermodynamic potentials to a non-equilibrium regime.

From Eqs. (12) and (17), the waste heat current is expressed using the non-equilibrium M-entropy as

$$\frac{d\tilde{Q}_A^{wst}(t)}{dt} = \frac{d\tilde{Q}_A^{ext}(t)}{dt} - \frac{d\Lambda_A^{neq}(t)}{dt}. \quad (18)$$

2. Nonequilibrium Helmholtz–Gibbs potentials

We introduce non-equilibrium Helmholtz and Gibbs energies defined as $F_A^{neq}(t) = -\Phi_A^{neq}(t)/\beta(t)$ and $G_A^{neq}(t) = -\Xi_A^{neq}(t)/\beta(t)$. Because $d\beta(t)/dt = -(1/k_B T^2(t))dT(t)/dt$, we obtain the time-derivative forms of these from Eqs. (14) and (15) as

$$\frac{dF_A^{neq}(t)}{dt} = -S_A^{neq}(t) \frac{dT(t)}{dt} + x(t) \frac{dX_A^{neq}(t)}{dt} + \frac{dQ_A^{wst}(t)}{dt} \quad (19)$$

and

$$\frac{dG_A^{neq}(t)}{dt} = -S_A^{neq}(t) \frac{dT(t)}{dt} + X_A^{neq}(t) \frac{dx(t)}{dt} + \frac{dQ_A^{wst}(t)}{dt}, \quad (20)$$

where $S_A^{neq}(t) = k_B \Lambda_A^{neq}(t)$ is a non-equilibrium entropy and we have introduced the waste heat current as

$$\frac{dQ_A^{wst}(t)}{dt} = \frac{1}{\beta(t)} \frac{d\tilde{Q}_A^{wst}(t)}{dt}. \quad (21)$$

From Eq. (16), we obtain the TDL transformation between the non-equilibrium Gibbs and Helmholtz potentials as

$$F_A^{neq}(t) = G_A^{neq}(t) + x(t)X_A^{neq}(t). \quad (22)$$

Solving Eq. (17) for $U_A^{neq}(t)$, we obtain the following TDL transformations:

$$U_A^{neq}(t) = F_A^{neq}(t) + T(t)S_A^{neq}(t). \quad (23)$$

From the above, we obtain the time-derivative expressions for the enthalpy and internal energy. The results

TABLE I. Time-derivative forms of the non-equilibrium (neq) Massieu–Planck potentials as functions of the intensive variables $\beta(t)$ and $\tilde{x}(t)$ and the extensive variables $U_A^{\text{neq}}(t)$ and $X_A^{\text{neq}}(t)$. Of the DL entropies, the commonly used one, which we call the Massieu entropy (M-entropy), involves only extensive variables and is denoted by $\Lambda_A^{\text{neq}}[U_A^{\text{neq}}(t), X_A^{\text{neq}}(t)]$, whereas the less widely used one, which we call the Planck entropy (P-entropy), is denoted by $\Gamma_A^{\text{qst}}[U_A^{\text{qst}}, \tilde{x}]$. Each potential is related to the others by the Legendre transformations shown in the final column.

| neq DL Thermodynamic pot. | Differential Form | Natural var. | Legendre Transformation |
|---------------------------|---|--------------------------------------|--|
| Massieu | $\frac{d}{dt}\Phi_A^{\text{neq}} = -U_A^{\text{neq}}\frac{d}{dt}\beta - \tilde{x}\frac{d}{dt}X_A^{\text{neq}} - \frac{d}{dt}Q_A^{\text{wst}}$ | β, X_A^{neq} | \dots |
| Planck | $\frac{d}{dt}\Xi_A^{\text{neq}} = -U_A^{\text{neq}}\frac{d}{dt}\beta + X_A^{\text{neq}}\frac{d}{dt}\tilde{x} - \frac{d}{dt}Q_A^{\text{wst}}$ | β, \tilde{x} | $\Xi_A^{\text{neq}} = \Phi_A^{\text{neq}} + \tilde{x}X_A^{\text{neq}}$ |
| M-Entropy | $\frac{d}{dt}\Lambda_A^{\text{neq}} = \beta\frac{d}{dt}U_A^{\text{neq}} - \tilde{x}\frac{d}{dt}X_A^{\text{neq}} - \frac{d}{dt}Q_A^{\text{wst}}$ | $U_A^{\text{neq}}, X_A^{\text{neq}}$ | $\Lambda_A^{\text{neq}} = \Phi_A^{\text{neq}} + \beta U_A^{\text{neq}}$ |
| P-Entropy | $\frac{d}{dt}\Gamma_A^{\text{neq}} = \beta\frac{d}{dt}U_A^{\text{neq}} + X_A^{\text{neq}}\frac{d}{dt}\tilde{x} - \frac{d}{dt}Q_A^{\text{wst}}$ | $U_A^{\text{neq}}, \tilde{x}$ | $\Gamma_A^{\text{neq}} = \Lambda_A^{\text{neq}} + \tilde{x}X_A^{\text{neq}}$ |

TABLE II. Time-derivative forms of the non-equilibrium (neq) Helmholtz–Gibbs potentials as functions of the intensive variables $T(t)$ and $x(t)$ and the extensive variables $S_A^{\text{neq}}(t)$ and $X_A^{\text{neq}}(t)$, which are interrelated through the Legendre transformations shown in the final column. Because heat is always lost in non-equilibrium processes, the waste heat $Q^{\text{wst}}(t)$ appears in the equations.

| neq Thermodynamic pot. | Differential Form | Natural var. | Legendre Transformation |
|------------------------|--|--------------------------------------|---|
| Helmholtz Energy | $\frac{d}{dt}F_A^{\text{neq}} = -S_A^{\text{neq}}\frac{d}{dt}T + x\frac{d}{dt}X_A^{\text{neq}} + \frac{d}{dt}Q_A^{\text{wst}}$ | T, x | $-$ |
| Gibbs Energy | $\frac{d}{dt}G_A^{\text{neq}} = -S_A^{\text{neq}}\frac{d}{dt}T - X_A^{\text{neq}}\frac{d}{dt}x + \frac{d}{dt}Q_A^{\text{wst}}$ | T, X_A^{neq} | $G_A^{\text{neq}} = F_A^{\text{neq}} - xX_A^{\text{neq}}$ |
| Internal Energy | $\frac{d}{dt}U_A^{\text{neq}} = T\frac{d}{dt}S_A^{\text{neq}} + x\frac{d}{dt}X_A^{\text{neq}} + \frac{d}{dt}Q_A^{\text{wst}}$ | S_A^{neq}, x | $U_A^{\text{neq}} = F_A^{\text{neq}} + TS_A^{\text{neq}}$ |
| Enthalpy | $\frac{d}{dt}H_A^{\text{neq}} = T\frac{d}{dt}S_A^{\text{neq}} - X_A^{\text{neq}}\frac{d}{dt}x + \frac{d}{dt}Q_A^{\text{wst}}$ | $S_A^{\text{neq}}, X_A^{\text{neq}}$ | $H_A^{\text{neq}} = U_A^{\text{neq}} - xX_A^{\text{neq}}$ |

are summarized in Table II. These results reduce to those in Table VI (Appendix A) in the quasi-static case. Thus, we can regard these potentials as extensions of the thermodynamic potentials to a non-equilibrium regime.

Dividing both sides of Eq. (3) by $\beta(t)$ yields the first law of thermodynamics expressed for the internal energy as

$$\frac{dU_A^{\text{neq}}(t)}{dt} = \frac{dW_A^{\text{ext}}(t)}{dt} + \frac{dQ_A^{\text{ext}}(t)}{dt}, \quad (24)$$

where

$$\frac{dQ_A^{\text{ext}}(t)}{dt} = \frac{1}{\beta(t)} \frac{d\tilde{Q}_A^{\text{ext}}(t)}{dt} \quad (25)$$

is the extensive heat current. From Eqs. (18) and (25), we can evaluate the DL waste heat current as

$$-\frac{d\tilde{Q}_A^{\text{wst}}(t)}{dt} = \frac{1}{k_B} \left\{ \frac{dS_A^{\text{neq}}(t)}{dt} - \frac{1}{T(t)} \frac{dQ_A^{\text{ext}}(t)}{dt} \right\}. \quad (26)$$

In the isothermal case, by integrating both sides between the two equilibrium states over time t , we obtain

$$-\tilde{Q}_A^{\text{wst}} = \frac{1}{k_B} \left\{ \Delta S_A^{\text{qst}} - \frac{Q_A^{\text{ext}}}{T} \right\}, \quad (27)$$

which indicates that the DL waste heat is equivalent to the entropy production evaluated for a heat engine.^{44,49}

The non-equilibrium Gibbs energy satisfies

$$S_A^{\text{neq}}(t) = - \left(\frac{\partial G_A^{\text{neq}}}{\partial T(t)} \right)_{x(t), \tilde{Q}_A^{\text{wst}}}, \quad (28)$$

$$X_A(t) = - \left(\frac{\partial G_A^{\text{neq}}}{\partial x(t)} \right)_{T(t), \tilde{Q}_A^{\text{wst}}}, \quad (29)$$

and

$$H_A(t) = -T^2(t) \frac{\partial}{\partial T(t)} \left(\frac{G_A^{\text{neq}}(t)}{T(t)} \right)_{x(t), \tilde{Q}_A^{\text{wst}}} \quad (30)$$

Equation (30) is an extension of the Gibbs–Helmholtz relation to a non-equilibrium regime.

III. NUMERICAL DEMONSTRATION

Although the results presented in Tables I and II hold for any non-equilibrium system consisting of subsystem and bath, the extensive variables and waste heat that appear in these relationships are system-specific, and there is no general theory on the basis of which non-equilibrium thermodynamic potentials can be obtained. However, it is possible to evaluate them as functions of the intensive and extensive variables using an optimization algorithm. Here, as a demonstration, we evaluate non-equilibrium thermodynamic potentials numerically using the thermodynamic SB model.⁵¹

A. Thermodynamic system–bath model

We employ the Ullersma–Caldeira–Leggett (or Brownian) model,^{24–26,59–62} which is ideal for thermodynamic simulations because the subsystem and bath are well defined, and rigorous numerical solutions can be obtained in both classical and quantum cases under any time-dependent external perturbation. Many of the favorable features for thermodynamic investigations arise from the presence of a counter term, which allows us to include the

contribution of the SB interaction in the bath.^{30–32,61–63} By introducing multiple heat baths at different temperatures controlled by time-dependent SB coupling functions, we can investigate isothermal, isentropic, thermostatic, and entropic processes. The total Hamiltonian for isothermal and thermostatic processes is written as⁵¹

$$\hat{H}_{\text{tot}}(t) = \hat{H}_A^0 + \hat{H}'_A(t) + \sum_{k=0}^N \hat{H}_{\text{IB}}^k(t), \quad (31)$$

where

$$\hat{H}_A^0 = \frac{\hat{p}^2}{2m} + U(\hat{q}) \quad (32)$$

is the unperturbed Hamiltonian of the subsystem with mass m and potential $U(\hat{q})$ described by momentum \hat{p} and position \hat{q} . The internal energy is then evaluated as $U_A^{\text{neq}}(t) = \text{tr}\{\hat{H}_A^0 \hat{\rho}_A(t)\}$, where $\hat{\rho}_A(t)$ is the reduced density operator of the subsystem. The external perturbation is expressed as $\hat{H}'_A(t) \equiv -x(t)\hat{X}_A$, where \hat{X}_A is an operator of the subsystem coordinate [i.e., $\hat{X}_A(\hat{q})$] and $x(t)$ is regarded as the thermodynamic intensive variable. The extensive variable is evaluated as $X_A^{\text{neq}}(t) = \text{tr}\{\hat{X}_A \hat{\rho}_A(t)\}$.

Although the conventional SB model has been limited to the investigation of isothermal processes at constant temperature, we can extend it to describe thermostatic processes in which temperature varies with time by introducing N independent heat baths, each in the thermal equilibrium state at the inverse temperature $\beta_k \equiv 1/k_B T_k$ connected to or disconnected from subsystem A using the window function $\xi_k(t)$.⁵¹ The k th bath Hamiltonian is expressed as an ensemble of harmonic oscillators and is given by

$$\hat{H}_{\text{IB}}^k(t) \equiv \sum_j \left\{ \frac{(\hat{p}_j^k)^2}{2m_j} + \frac{m_j^k (\omega_j^k)^2}{2} \left[\hat{x}_j^k - \frac{c_j^k A_k \xi_k(t) \hat{q}}{m_j^k (\omega_j^k)^2} \right]^2 \right\}, \quad (33)$$

where the momentum, position, mass, and frequency of the j th bath oscillator are given by \hat{p}_j^k , \hat{x}_j^k , m_j^k , and ω_j^k , respectively. Here, we consider the situation where N independent heat baths, each in the thermal equilibrium state $\exp(-\beta_k \hat{H}_{\text{IB}}^k)$ at the inverse temperature $\beta_k \equiv 1/k_B T_k$, are connected or disconnected to subsystem A according to a control function $\xi_k(t)$. The bath temperature is effectively expressed as

$$T(t) = \sum_{k=1}^N T_k \xi_k(t), \quad (34)$$

or the inverse temperature as $\beta(t) = [k_B T(t)]^{-1}$. As a spectral distribution function for the k th bath $J^k(\omega) \equiv \sum_j \hbar (c_j^k A_k)^2 / (2m_j^k) \omega_j^k \delta(\omega - \omega_j^k)$, we consider the Ohmic case described by

$$J^k(\omega) = \frac{\hbar A_k^2 \omega}{\pi} \quad (35)$$

and assume that the time scale of the quantum thermal fluctuations $\beta(t)\hbar/2\pi$ is shorter than the time scale of the external perturbations $\beta(t)$ and $x(t)$. This allows us to extend the low-temperature quantum Fokker–Planck equations (LT-QFPE)⁵² for the set of Wigner distribution functions $W_{\vec{n}}(p, q; t)$, where \vec{n} is the index of hierarchy member, and the Kramers equation for phase space distribution function $W(p, q; t)$ to apply the thermostatic case by introducing time-dependent Matsubara frequencies $\nu(t) = 1/\hbar\beta(t)$. Expressions for these equations are presented in Ref. 51. The source code for thermodynamic HEOM in phase space representation and thermodynamic Kramers equation are provided as a separated paper.⁶⁴

It should be noted that in the non-Ohmic case, the temperature may change even on the time scale on which the noise correlations are defined. This makes it difficult to apply the fluctuation–dissipation theorem to characterize the noise, and thus a simple replacement $\beta \rightarrow \beta(t)$ is not allowed.

B. DL work and extensive variables

We express the solution for the reduced density elements under any $x(t)$ in the Wigner representation using the zeroth member of the hierarchical Wigner functions as $W(p, q, t) \equiv W_0(p, q, t)$. In the classical limit $\hbar \rightarrow 0$, $W(q, p; t)$ corresponds to the classical distribution function. We use this to define the change in DL intensive work over time corresponding to power and heat flow as follows:

$$\frac{d\tilde{W}_A^{\text{int}}(t)}{dt} = U_A^{\text{neq}}(t) \frac{d\beta(t)}{dt} - X_A^{\text{neq}}(t) \frac{d\tilde{x}(t)}{dt}, \quad (36)$$

where the extensive variables in the Wigner representation at time t are expressed as

$$X_A^{\text{neq}}(t) = \text{tr}_A \{X_A(q)W(p, q; t)\} \quad (37)$$

and

$$U_A^{\text{neq}}(t) = \text{tr}_A \left\{ \left[\frac{p^2}{2m} + U(q) \right] W(p, q; t) \right\}. \quad (38)$$

From the definition (2) of extensive work and the TDL transformations (6) and (7), the extensive heat current is evaluated as

$$\frac{dQ_A^{\text{ext}}(t)}{dt} = \text{tr}_A \left\{ \left[\frac{p^2}{2m} + U(q) - x(t)X_A(q) \right] \frac{\partial W(p, q; t)}{\partial t} \right\}. \quad (39)$$

C. Evaluation of the non-equilibrium Planck potential

From Eq. (B1), we obtain the expression for the non-equilibrium Planck potential $(\Xi_A^{\text{neq}})_k = \Xi_A^{\text{neq}}[\beta(t_k), \tilde{x}(t_k)]$

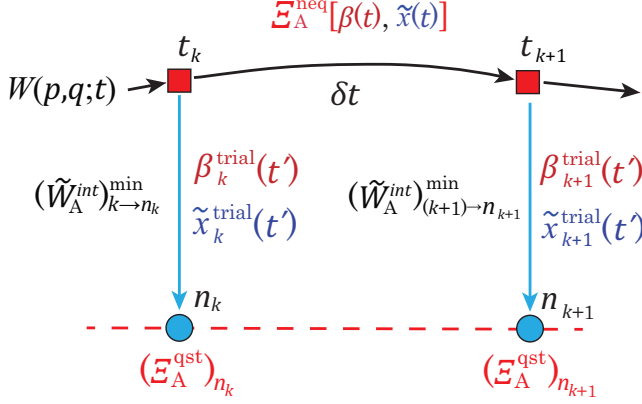


FIG. 1. Schematic of the evaluation of the non-equilibrium Planck potential $\Xi_A^{\text{neq}}(t)$ at t_k and t_{k+1} . A non-equilibrium process driven by the intensive variables $\beta(t)$ and $\tilde{x}(t)$ is described as the non-equilibrium distribution $W(p, q; t)$ expressed by the black arrows. The equilibrium states for different sets of β_k^{qst} and \tilde{x}_k^{qst} are expressed by the red dashed line. For each state k to the equilibrium state n_k , we minimize $(\tilde{W}_A^{\text{int}})_{k \rightarrow n_k} + (\Xi_A^{\text{qst}})_{n_k}$ by choosing the trial functions $\beta_k^{\text{trial}}(t')$ and $\tilde{x}_k^{\text{trial}}(t')$, where $(\tilde{W}_A^{\text{int}})_{k \rightarrow n_k}^{\text{min}}$ is the DL minimum intensive work for $k \rightarrow n_k$ and $(\Xi_A^{\text{qst}})_{n_k}$ is the quasi-static Planck potential at the state n_k . We can then evaluate the non-equilibrium Planck potential at the state k as $(\Xi_A^{\text{neq}})_k = (\tilde{W}_A^{\text{int}})_{k \rightarrow n_k}^{\text{min}} + (\Xi_A^{\text{qst}})_{n_k}$.

of the non-equilibrium-to-equilibrium process $k \rightarrow n_k$ as

$$(\Xi_A^{\text{neq}})_k = (\tilde{W}_A^{\text{int}})_{k \rightarrow n_k}^{\text{min}} + (\Xi_A^{\text{qst}})_{n_k}, \quad (40)$$

where n_k represents an equilibrium state, $(\tilde{W}_A^{\text{int}})_{k \rightarrow n_k}^{\text{min}}$ is the DL minimum intensive work for $k \rightarrow n_k$, and $(\Xi_A^{\text{qst}})_{n_k}$ is the quasi-static Planck potential at state n_k . As shown in Eq. (B5), because the right-hand side of Eq. (40) is independent of the choice of n_k , to evaluate $(\Xi_A^{\text{neq}})_k$, we do not specify n_k to minimize $(\tilde{W}_A^{\text{int}})_{k \rightarrow n_k} + (\Xi_A^{\text{qst}})_{n_k}$.

To perform numerical calculations, we express Eq. (40) with Eq. (15) in terms of trial functions $\beta^{\text{trial}}(t_k, t')$ and $\tilde{x}^{\text{trial}}(t_k, t')$ as

$$Xi_A^{\text{target}}[\beta^{\text{trial}}(t), \tilde{x}^{\text{trial}}(t)] = \Xi_A^{\text{qst}}(\beta_{n_k}^{\text{qst}}, \tilde{x}_{n_k}^{\text{qst}}) + \int_t^{t+\Delta t} \left[U_A(t') \frac{d\beta^{\text{trial}}(t')}{dt'} - X_A(t') \frac{d\tilde{x}^{\text{trial}}(t')}{dt'} \right] dt', \quad (41)$$

where $\Xi_A^{\text{target}}[\beta^{\text{trial}}(t), \tilde{x}^{\text{trial}}(t)]$ is the target function to be minimized and $\Xi_A^{\text{qst}}(\beta_{n_k}^{\text{qst}}, \tilde{x}_{n_k}^{\text{qst}})$ is the quasi-static Planck potential at n_k , which is also evaluated from the LT-QFPE and Kramers equation. The DL trail function $\tilde{x}_k^{\text{trial}}(t)$ in Eq. (41) is evaluated from $x_k^{\text{trial}}(t)$ as $\tilde{x}_k^{\text{trial}}(t) = \beta_k^{\text{trial}}(t)x_k^{\text{trial}}(t)$. To reduce the computational cost, we assume that the optimized trial functions become constant after the characteristic time for the equilibration Δt , as $\beta_{n_k}^{\text{qst}} = \beta_k^{\text{trial}}(t_k + \Delta t)$ and $\tilde{x}_{n_k}^{\text{qst}} = \tilde{x}_k^{\text{trial}}(t_k + \Delta t)$.

As the trial functions for time $t' > t_k$, we chose the N_β th and N_x th Taylor expansion forms expressed as

$$\beta_k^{\text{trial}}(t') = \sum_{n=0}^{N_\beta} \beta_k^{(n)}(t' - t_k)^n, \quad (42)$$

and

$$x_k^{\text{trial}}(t') = \sum_{n=0}^{N_x} x_k^{(n)}(t' - t_k)^n, \quad (43)$$

where $\beta_k^{(n)}$ and $x_k^{(n)}$ are the n th-order Taylor coefficients. Thus, the functional minimization of $\Xi_A^{\text{target}}[\beta^{\text{trial}}(t), \tilde{x}^{\text{trial}}(t)]$ becomes a multivariable function minimization for $\beta_k^{(n)}$ and $x_k^{(n)}$.

Then, $\Xi_A^{\text{neq}}(t)$ is evaluated as follows (see Fig. 1). First, we perform the non-equilibrium simulations for given $\beta(t)$ and $\tilde{x}(t)$ to obtain $W_{\tilde{n}}(p, q; t)$ for each t_k . The minimum work from the non-equilibrium state k to the equilibrium state n_k expressed as $(\tilde{W}_A^{\text{int}})_{k \rightarrow n_k}^{\text{min}}$ is then evaluated using an optimization algorithm for $\beta_k^{\text{trial}}(t')$ and $\tilde{x}_k^{\text{trial}}(t')$. From Eq. (40), we set this value as $(\Xi_A^{\text{neq}})_k$. By repeating this procedure for different values of k , we obtain $\Xi_A^{\text{neq}}(t_k)$ at each step. The other potentials can be evaluated from the TDL transformations.

D. Quantum and classical Stirling engine

The non-equilibrium thermodynamic potentials are state variables as functions of the non-equilibrium intensive and extensive variables, which are also state variables, while Q_A^{wst} is not, and, in the quasi-static limit, they reduce to conventional thermodynamic potentials. These non-equilibrium potentials are useful because they can be used to analyze thermodynamic processes using work diagrams, as in the case of equilibrium thermodynamics. By finding a thermodynamic process to minimize waste heat, we can construct a heat machine with maximum efficiency under non-equilibrium conditions, although the efficiency is lower than the Carnot limit.^{49,50}

Here, we demonstrate how to evaluate non-equilibrium potentials for a case in which $\beta(t)$ and $x(t)$ are specified. For this purpose, we consider the classical/quantum Stirling engine (CSE/QSE) consisting of four steps: (i) a hot isothermal process, (ii) a transition from a hot to cold thermostatic process, (iii) a cold isothermal process, and (iv) a transition from a cold to hot thermostatic process for an anharmonic potential system. Since the purpose of the calculation is to illustrate how the potentials are calculated, we fix the changes in $\beta(t)$ and $x(t)$ as shown in Fig. 2 with $\tau = 20$ and do not optimize them to improve their efficiency.

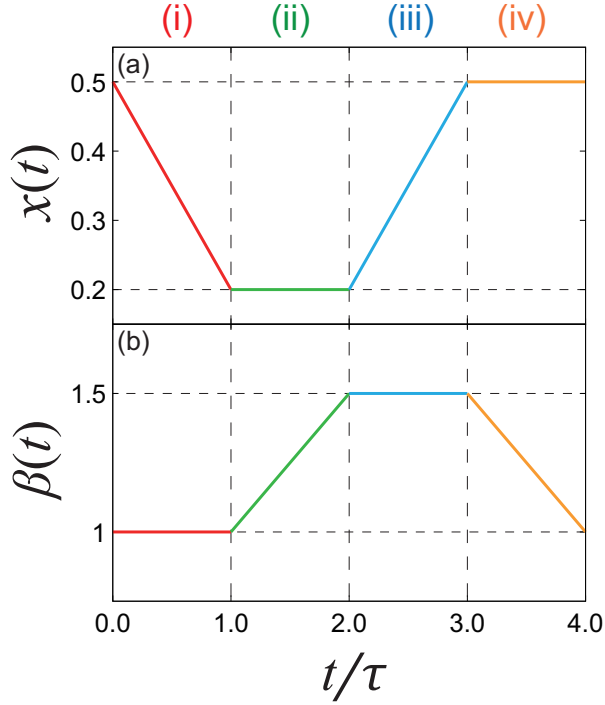


FIG. 2. Time profiles of (a) the electric field $x(t)$ and (b) the inverse temperature $\beta(t)$ for the Stirling engine. The red, green, blue, and orange lines represent (i) hot isothermal, (ii) isoelectric (from hot to cold), (iii) cold isothermal, and (iv) isoelectric (from cold to hot) processes, respectively. Time t is normalized by the period of the cycle τ .

1. Simulation details

We performed simulations using the anharmonic potential system employed in our previous study.⁵¹ Thus, we considered a quartic anharmonic potential with the external interaction described as $X_A(\hat{q}) = \hat{q}$. The potential function in Eq. (32) is expressed as

$$U(\hat{q}) = U_2\hat{q}^2 + U_3\hat{q}^3 + U_4\hat{q}^4, \quad (44)$$

where the constants are given by $U_2 = 0.1$, $U_3 = 0.02$, and $U_4 = 0.05$. Numerical calculations were carried out to integrate the thermodynamic HEOM in the quantum cases and the thermodynamic Kramers equation in the classical cases. The detailed conditions for the numerical calculations, including the working parameters, are presented in Table III and in Ref. 51

To set the trial functions defined in Eqs. (42) and (43), we chose $N_\beta = N_x = 5$. Then, using the Nelder-Mead method, we minimized $\Xi_A^{\text{target}}[\beta^{\text{trial}}(t), x^{\text{trial}}(t)]$ in Eq. (41) with a cutoff time $\Delta t = 1.0$. We evaluated $\Xi_A^{\text{neq}}(t)$ every 20 steps. The value of the quasi-static Planck potential $\Xi_A^{\text{qst}}(\beta^{\text{qst}}, \hat{x}^{\text{qst}})$ in Eq. (41) was obtained by integrating the thermodynamic LT-QFPE and the Kramers equation.

TABLE III. Parameter values used for the simulations of the Stirling engine. Here, dx and dp are the mesh sizes for position and momentum, respectively, in Wigner space. The integers N and K are the cutoff numbers used in the LT-FPE.

| | A | N | K | dx | dp |
|-----------|---------|-----|-----|------|------|
| Classical | 0.5–1.5 | ... | ... | 0.25 | 0.25 |
| Quantum | 0.5 | 6 | 2 | 0.3 | 0.4 |
| | 1.0 | 7 | 2 | 0.3 | 0.5 |
| | 1.5 | 8 | 2 | 0.3 | 0.6 |

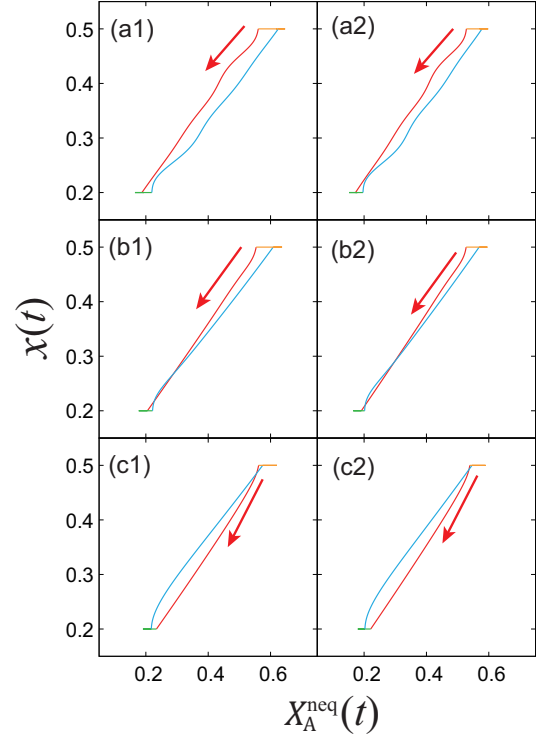


FIG. 3. $x(t)$ - $X_A^{\text{neq}}(t)$ diagrams for the Stirling engine in the classical case (1, left column) and quantum case (2, right column) for (a) $A = 0.5$ (weak), (b) 1.0 (intermediate), and (c) 1.5 (strong) SB coupling strengths. In each plot, the four curves (or lines) represent (i) hot isothermal (red), (ii) from hot to cold thermostatic (green), (iii) cold isothermal (blue), and (iv) from cold to hot thermostatic (orange) processes, respectively. The processes evolve in a counterclockwise fashion over time in a heat engine, whereas they evolve in a clockwise fashion over time in a refrigerator.

2. Results

The extensive variables $X_A^{\text{neq}}(t)$ and $U_A^{\text{neq}}(t)$ were obtained from Eqs. (37) and (38), respectively. The non-equilibrium entropy expressed as $S_A^{\text{neq}}(t) = k_B \Lambda_A^{\text{neq}}(t)$ was then obtained from $X_A^{\text{neq}}(t)$, and $U_A^{\text{neq}}(t)$ and $\Xi_A^{\text{neq}}(t)$ were evaluated according to the procedure described in Sec. III C using the TDL transformations Eqs. (16) and

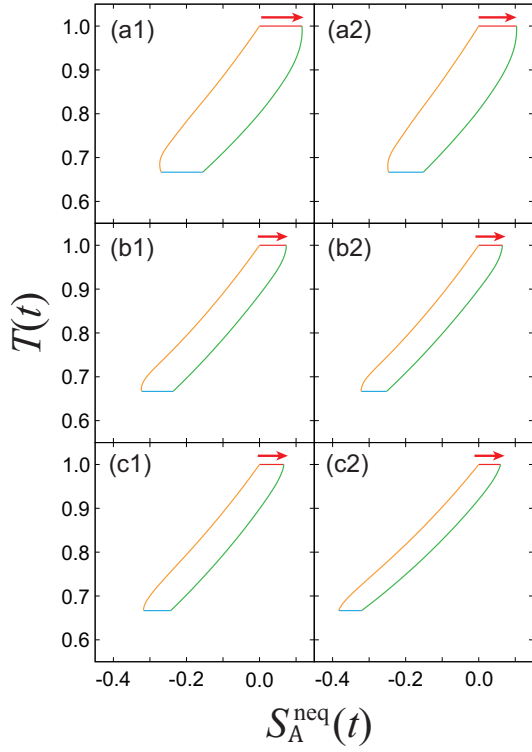


FIG. 4. $T(t)$ - $S_A^{\text{neq}}(t)$ diagrams for the Stirling engine in the classical case (1, left column) and quantum case (2, right column) for (a) $A = 0.5$ (weak), (b) 1.0 (intermediate), and (c) 1.5 (strong) SB coupling strength, respectively. Each cycle starts with the red arrow, and the four curves represent (i) hot isothermal (red), (ii) from hot to cold thermostatic (green), (iii) cold isothermal (blue), and (iv) from cold to hot thermostatic (orange) processes, respectively.

TABLE IV. Work performed in one cycle for the classical and quantum cases for different SB coupling strengths.

| A | W (classical) | W (quantum) |
|--------------------|------------------------|------------------------|
| 0.5 (weak) | -1.44×10^{-2} | -1.07×10^{-2} |
| 1.0 (intermediate) | -5.77×10^{-3} | -3.09×10^{-3} |
| 1.5 (strong) | 1.01×10^{-2} | 1.10×10^{-2} |

(17). The results are depicted as non-equilibrium $x(t)$ - $X_A^{\text{neq}}(t)$ and $T(t)$ - $S_A^{\text{neq}}(t)$ diagrams, which are closed because the cycle is steady and because $T(t)$, $S_A^{\text{neq}}(t)$, $x(t)$, and $X_A^{\text{neq}}(t)$ are state variables.

We first present the $x(t)$ - $X_A^{\text{neq}}(t)$ diagrams for weak ($A = 0.5$), intermediate ($A = 1.0$), and strong ($A = 1.5$) system-bath coupling strengths in Fig. 3. The area enclosed by each diagram corresponds to positive work when evolving in the counterclockwise direction over time, whereas it corresponds to negative work when evolving clockwise. The work performed in one cycle is presented in Table IV. In each diagram in Fig. 3, the red and blue horizontal lines appear because there is a time

delay in the change of $X_A^{\text{neq}}(t)$ with respect to $x(t)$ for the heat bath to take effect.

As shown in Fig. 3 and Table IV, the larger the SB coupling, the smaller the quantum effect, because it is suppressed by relaxation.⁵² Thus, when the coupling is large, dissipation becomes dominant, and the system becomes a refrigerator (or damper). This is because the time scales of fluctuations and dissipation are different: in the non-equilibrium case, dissipation dominates when the SB coupling is large, whereas in the quasi-static case, fluctuations and dissipation are balanced regardless of the coupling strength. This is a distinct difference from the Carnot case; the efficiency reaches a maximum in the intermediate SB coupling region where A is neither large nor small.⁷

Next, we present the $T(t)$ - $S_A^{\text{neq}}(t)$ diagrams in Fig. 4. The area enclosed by a clockwise curve represents the difference between extensive heat and waste heat, $Q_A^{\text{ext}} - Q_A^{\text{wst}}$, per cycle. In the quasi-static case, the area agrees with the extensive heat per cycle because Q_A^{wst} becomes zero. In the thermostatic processes (green and orange curves), when the SB coupling is small, there is a time delay in the change of $S_A^{\text{neq}}(t)$ with respect to $T(t)$. This occurs because it takes time for the system to be excited when thermal fluctuations are small, whereas the delay is almost negligible when the SB coupling is strong.

In Fig. 5, we show the (time-averaged) waste heat current, enthalpy, and internal energy as functions of t . As we show in Sec. II, the waste heat current is always negative, and it becomes large in the isothermal case for larger SB coupling because of the strong dissipation, whereas it becomes small in the thermostatic processes for the case of weak SB coupling because fluctuations are suppressed.

Using the graph of the waste heat current, we can improve the cycle efficiency. For instance, in the case of strong coupling, because a large waste heat current occurs in the isothermal processes, by increasing the duration of the isothermal processes, we can reduce the waste heat in the cycle.

For weak SB coupling, both the enthalpy and internal energy in the classical case agree with those in the quantum case, whereas for strong SB coupling, they disagree, owing to the quantum coherence between the system and bath (bathentanglement).³¹

IV. CONCLUSIONS

The virtue of thermodynamics lies in its ability to describe, in a system-independent manner, macroscopic thermal phenomena resulting from complex microscopic interactions as changes in thermodynamic potentials described as interrelated intensive and extended variables through Legendre transformations.

We have developed the laws of thermodynamics as applied to work in a system-independent manner, based on the principle of DL minimum work. Subsequently, we have developed a non-equilibrium thermodynamic the-

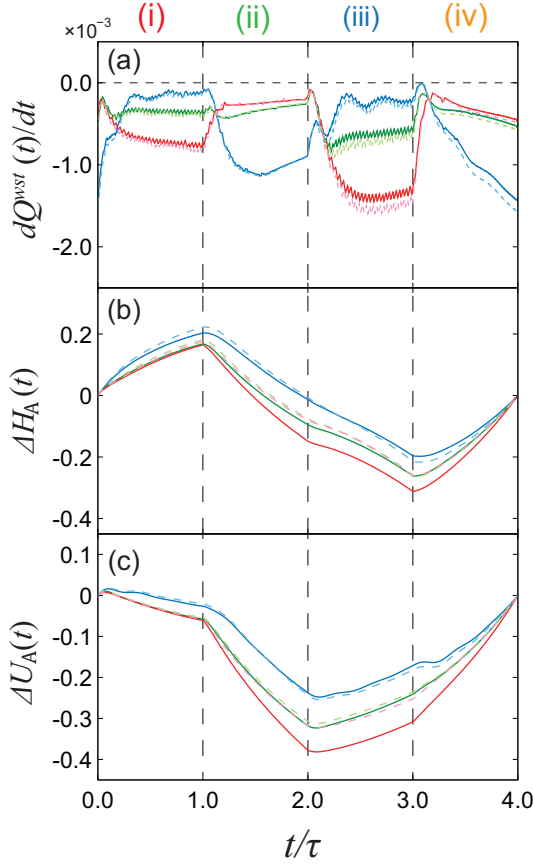


FIG. 5. (a) Waste heat current $dQ^{\text{wst}}(t)/dt$, (b) enthalpy, and (c) internal energy as functions of t . The blue, green, and red curves represent the weak ($A = 0.5$), intermediate ($A = 1.0$), and strong ($A = 1.5$) SB coupling cases, respectively. The solid and dashed curves represent the quantum and classical results, respectively. The plots of waste heat currents have been time-averaged over 10 steps each using the raw data.

ory that describes non-equilibrium thermodynamic potential in terms of time-dependent intensive and extensive variables, along with waste heat.

Thus, the non-equilibrium Massieu-Planck and Helmholtz-Gibbs potentials are obtained in time-derivative form in terms of non-equilibrium extensive and intensive variables, which are state variables along with waste heat, which is not a state variable. Our results are summarized in Tables I and II and are consistent with traditional thermodynamics in a quasi-static case, as presented in Tables V and VI.

These results have been validated for quantum and classical Stirling engines through numerical simulations based on the thermodynamic SB model, which can describe both isothermal and thermostatic processes. An optimization algorithm has been used to evaluate non-equilibrium thermodynamic potentials. Work diagrams in non-equilibrium regimes have been presented and analyzed.

Although the time evolution of the system in the non-

equilibrium regime is model-specific, it is possible to test our theory even in real systems through the use of optimization algorithms. By designing processes to reduce waste heat, it may be possible to develop efficient heat engines even for non-equilibrium processes.

In engineering, the effective energy from non-equilibrium to equilibrium is referred to as exergy.^{57,58} The non-equilibrium thermodynamic potentials we have introduced can be regarded as a generalization of it. The present theory provides a methodology to systematically evaluate and improve it, which should be useful from the perspective of Sustainable Development Goal (SDGs).

ACKNOWLEDGMENTS

The authors thank Yoshi Oono for his critical comments on the definition and terminology of thermodynamic variables, particularly for extensive variables. Y.T. was supported by JSPS KAKENHI (Grant No. B21H01884). S.K. was supported by JST fellowship, the establishment of university fellowships towards the creation of science technology innovation (Grant No. JPMJFS2123), and by Grant-in-Aid for JSPS Fellows (Grant No. 24KJ1373).

AUTHOR DECLARATIONS

Conflict of Interest

The authors have no conflicts to disclose.

DATA AVAILABILITY

The data that support the findings of this study are available from the corresponding author upon reasonable request.

Appendix A: Quasi-static thermodynamic potentials

We introduce the DL intensive heat defined as

$$\frac{d\tilde{Q}_A^{\text{int}}(t)}{dt} \equiv \beta(t) \frac{dU_A(t)}{dt} + X_A(t) \frac{d\tilde{x}(t)}{dt} \quad (\text{A1})$$

which satisfies the Legendre transformation

$$\frac{d\tilde{Q}_A^{\text{int}}(t)}{dt} = \frac{d\tilde{Q}_A^{\text{ext}}(t)}{dt} + \frac{d}{dt} [\tilde{x}(t)X_A(t)]. \quad (\text{A2})$$

The extensive and intensive work and heat $\tilde{W}_A^{\text{ext}}(t)$, $\tilde{W}_A^{\text{int}}(t)$, $\tilde{Q}_A^{\text{ext}}(t)$, and $\tilde{Q}_A^{\text{int}}(t)$ are interrelated through the Legendre transformations (6), (7), and (A2). Therefore, the inequalities (8), (9),

$$\tilde{W}_A^{\text{int}} \geq -\Delta\Xi_A^{\text{qst}}, \quad (\text{A3})$$

TABLE V. Total differential expressions for the quasi-static (qst.) entropic potentials as functions of the intensive variables $\beta^{\text{qst}}(t)$ and $\tilde{x}^{\text{qst}}(t)$ and the extensive variables $U_A^{\text{qst}}(t)$ and $X_A^{\text{qst}}(t)$. Entropy has two definitions, depending on whether the work variable is intensive or extensive. Of these DL entropies, the commonly used one, which we call Massieu entropy (M-entropy), involves only extensive variables and is denoted by $\Lambda_A^{\text{qst}}[U_A^{\text{qst}}, X_A^{\text{qst}}]$, whereas the less widely used one, which we call Planck entropy (P-entropy), is denoted by $\Gamma_A^{\text{qst}}[U_A^{\text{qst}}, \tilde{x}^{\text{qst}}]$. Whereas the enthalpy $H_A^{\text{qst}}(t)$ was chosen as the natural variable in Ref. 51, here we chose the internal energy U_A^{qst} instead. Each potential is related to the others by the Legendre transformations shown in the final column.

| Qst. Potential | Differential form | Natural var. | Legendre transformation |
|----------------|---|--|--|
| Massieu | $d\Phi_A^{\text{qst}} = -U_A^{\text{qst}} d\beta^{\text{qst}} - \tilde{x}^{\text{qst}} dX_A^{\text{qst}}$ | $\beta^{\text{qst}}, X_A^{\text{qst}}$ | \dots |
| Planck | $d\Xi_A^{\text{qst}} = -U_A^{\text{qst}} d\beta^{\text{qst}} + X_A^{\text{qst}} d\tilde{x}^{\text{qst}}$ | $\beta^{\text{qst}}, \tilde{x}^{\text{qst}}$ | $\Xi_A^{\text{qst}} = \Phi_A^{\text{qst}} + \tilde{x}^{\text{qst}} X_A^{\text{qst}}$ |
| M-Entropy | $d\Lambda_A^{\text{qst}} = \beta^{\text{qst}} dU_A^{\text{qst}} - \tilde{x}^{\text{qst}} dX_A^{\text{qst}}$ | $U_A^{\text{qst}}, X_A^{\text{qst}}$ | $\Lambda_A^{\text{qst}} = \Xi_A^{\text{qst}} + \beta^{\text{qst}} U_A^{\text{qst}}$ |
| P-Entropy | $d\Gamma_A^{\text{qst}} = \beta^{\text{qst}} dU_A^{\text{qst}} + X_A^{\text{qst}} d\tilde{x}^{\text{qst}}$ | $U_A^{\text{qst}}, \tilde{x}^{\text{qst}}$ | $\Gamma_A^{\text{qst}} = \Phi_A^{\text{qst}} + \beta^{\text{qst}} U_A^{\text{qst}}$ |

and

$$\tilde{Q}_A^{\text{int}} \leq \Delta\Gamma_A^{\text{qst}}, \quad (\text{A4})$$

where Γ_A^{qst} is the Planck entropy (P-entropy), are all expressions of the second law of thermodynamics.

The total differential forms of the Massieu–Planck potentials are presented in Table V.

The Helmholtz–Gibbs potentials can be obtained from the Massieu–Planck potentials using the definitions $F_A^{\text{qst}}(t) = -\Phi_A^{\text{qst}}(t)/\beta^{\text{qst}}(t)$ and $G_A^{\text{qst}}(t) = -\Xi_A^{\text{qst}}(t)/\beta^{\text{qst}}(t)$. From Eq. (6), we have

$$F_A^{\text{qst}}(t) = G_A^{\text{qst}}(t) + x^{\text{qst}}(t)X_A^{\text{qst}}(t). \quad (\text{A5})$$

Accordingly, from Eq. (7), we have

$$U_A^{\text{qst}}(t) = F_A^{\text{qst}}(t) + T^{\text{qst}}(t)S_A^{\text{qst}}(t), \quad (\text{A6})$$

where we have used $d\beta^{\text{qst}}(t)/dt = -(1/k_B[T^{\text{qst}}(t)]^2)dT^{\text{qst}}(t)/dt$ and $S_A^{\text{qst}}(t) = k_B\Lambda_A^{\text{qst}}(t)$.

The total differential forms of the Helmholtz–Gibbs potentials are presented in Table VI.

Appendix B: DL non-equilibrium minimum work principle

Here, we derive fundamental equations to develop the DL non-equilibrium minimum work principle. Consider two equilibrium states 1 and 2 that are connected by a quasi-static process (see Fig. 6). From the principle of DL minimum work [Eq. (8)], the work done in this process is equivalent to the difference in Massieu potentials: $(\tilde{W}_A^{\text{ext}})^{\text{min}}_{1 \rightarrow 2} = -(\Delta\Phi_A^{\text{qst}})_{1 \rightarrow 2} \equiv (\Phi_A^{\text{qst}})_1 - (\Phi_A^{\text{qst}})_2$, where $n \rightarrow n'$ represents the transition from any state n to n' . Separately, we consider the non-equilibrium state A and introduce the non-equilibrium process $1 \rightarrow A$ (dark blue curve in Fig. 6), and any process from A to 2 (green and light blue curves). For each of these processes, the work done is denoted by $(\tilde{W}_A^{\text{ext}})_{1 \rightarrow A}$ and $(\tilde{W}_A^{\text{ext}})_{A \rightarrow 2}$, respectively. For fixed $(\tilde{W}_A^{\text{ext}})_{1 \rightarrow A}$, the value of $(\tilde{W}_A^{\text{ext}})_{A \rightarrow 2}$ changes depending on the path.

From the second law of thermodynamics [Eq. (8)], we then have $(\tilde{W}_A^{\text{ext}})_{1 \rightarrow A} + (\tilde{W}_A^{\text{ext}})_{A \rightarrow 2} > -(\Delta\Phi_A^{\text{qst}})_{1 \rightarrow 2}$.

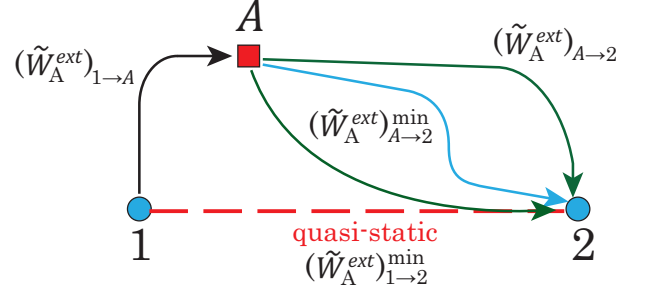


FIG. 6. Schematic to derive Eq. (B1). The blue circles 1 and 2 represent the equilibrium states, and the red square A represents the non-equilibrium state. The quasi-static work performed for $1 \rightarrow 2$ (red dashed line) is denoted by $(\tilde{W}_A^{\text{ext}})^{\text{min}}_{1 \rightarrow 2}$, while the non-equilibrium work from 1 to A (dark blue curve) is denoted by $(\tilde{W}_A^{\text{ext}})_{1 \rightarrow A}$. When $(\tilde{W}_A^{\text{ext}})_{1 \rightarrow A}$ is fixed, the value of $(\tilde{W}_A^{\text{ext}})_{A \rightarrow 2}$ depends on the path (green and light blue curves). From the second law of thermodynamics, we have $(\tilde{W}_A^{\text{ext}})_{1 \rightarrow A} + (\tilde{W}_A^{\text{ext}})_{A \rightarrow 2} \geq -(\Delta\Phi_A^{\text{qst}})_{1 \rightarrow 2}$. This indicates a lower bound of work for $A \rightarrow 2$ denoted by $(\tilde{W}_A^{\text{ext}})^{\text{min}}_{A \rightarrow 2}$ (light blue curve) and given by Eq. (B1).

This indicates that $(\tilde{W}_A^{\text{ext}})_{A \rightarrow 2}$ has a lower bound for fixed $(\tilde{W}_A^{\text{ext}})_{1 \rightarrow A}$; otherwise the inequality is violated, for example, as $-\infty > -(\Delta\Phi_A^{\text{qst}})_{1 \rightarrow 2} - (\tilde{W}_A^{\text{ext}})_{1 \rightarrow A}$. Using the lower bound of the work, we introduce the non-equilibrium Massieu potential Φ_A^{neq} defined as

$$(\tilde{W}_A^{\text{ext}})^{\text{min}}_{A \rightarrow 2} = -[(\Phi_A^{\text{qst}})_2 - (\Phi_A^{\text{neq}})_A]. \quad (\text{B1})$$

Introducing a second non-equilibrium state B on the pathway $A \rightarrow 2$ as depicted in Fig. 7, we now discuss the non-equilibrium transition $A \rightarrow B$ (red arrow). We consider the non-equilibrium-to-equilibrium minimum work from B to 2 (light blue curve), expressed as

$$(\tilde{W}_A^{\text{ext}})^{\text{min}}_{B \rightarrow 2} = -[(\Phi_A^{\text{qst}})_2 - (\Phi_A^{\text{neq}})_B]. \quad (\text{B2})$$

From the inequality $(\tilde{W}_A^{\text{ext}})_{A \rightarrow 2} \geq -[(\Phi_A^{\text{qst}})_2 - (\Phi_A^{\text{neq}})_A]$ and Eq. (B2), we have

$$(\tilde{W}_A^{\text{ext}})_{A \rightarrow B} \geq -(\Delta\Phi_A^{\text{neq}})_{A \rightarrow B}, \quad (\text{B3})$$

TABLE VI. Total differential expressions for the quasi-static (qst.) thermodynamic potentials as functions of the intensive variables $T^{\text{qst}}(t)$ and $x^{\text{qst}}(t)$ and the extensive variables $S_A^{\text{qst}}(t)$ and $X_A^{\text{qst}}(t)$, which are related through the Legendre transformations shown in the final column.⁵¹

| Qst. potential | Differential form | Natural var. | Legendre transformation |
|----------------|--|--------------------------------------|---|
| Helmholtz | $dF_A^{\text{qst}} = -S_A^{\text{qst}} dT^{\text{qst}} + x_A^{\text{qst}} dX_A^{\text{qst}}$ | $T^{\text{qst}}, X_A^{\text{qst}}$ | \dots |
| Gibbs | $dG_A^{\text{qst}} = -S_A^{\text{qst}} dT^{\text{qst}} - X_A^{\text{qst}} dx_A^{\text{qst}}$ | $T^{\text{qst}}, x_A^{\text{qst}}$ | $G_A^{\text{qst}} = F_A^{\text{qst}} - x_A^{\text{qst}} X_A^{\text{qst}}$ |
| Internal | $dU_A^{\text{qst}} = T^{\text{qst}} dS_A^{\text{qst}} + x_A^{\text{qst}} dX_A^{\text{qst}}$ | $S_A^{\text{qst}}, X_A^{\text{qst}}$ | $U_A^{\text{qst}} = F_A^{\text{qst}} + T^{\text{qst}} S_A^{\text{qst}}$ |
| Enthalpy | $dH_A^{\text{qst}} = T^{\text{qst}} dS_A^{\text{qst}} - X_A^{\text{qst}} dx_A^{\text{qst}}$ | $S_A^{\text{qst}}, x_A^{\text{qst}}$ | $H_A^{\text{qst}} = G_A^{\text{qst}} + T^{\text{qst}} S_A^{\text{qst}}$ |

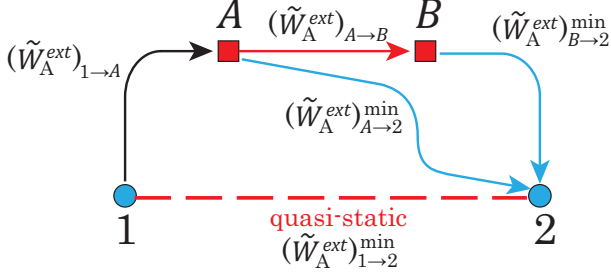


FIG. 7. Schematic to derive the principle of DL non-equilibrium minimum work expressed by Eq. (B3). We consider two non-equilibrium states A and B (red square) that are connected by a non-equilibrium process described by the red arrow for $A \rightarrow B$. The light blue curves $A \rightarrow 2$ and $B \rightarrow 2$ represent non-equilibrium-to-equilibrium minimum work paths whose work is denoted by $(\tilde{W}_A^{\text{ext}})_{A \rightarrow 2}^{\min}$ and $(\tilde{W}_A^{\text{ext}})_{B \rightarrow 2}^{\min}$, respectively.

where $(\tilde{W}_A^{\text{ext}})_{A \rightarrow B} \equiv (\tilde{W}_A^{\text{ext}})_{A \rightarrow 2} - (\tilde{W}_A^{\text{ext}})_{B \rightarrow 2}^{\min}$. Thus, equality holds in (B3) when B is on the minimal pathway ($A \rightarrow 2$)^{min}.

Because a non-equilibrium process changes as a function of time, it is more convenient to use the time-derivative form of the above. Thus, for the process from A to B at times t and $t + dt$, where dt is an infinitesimal time, we have the following inequality:

$$\frac{d\tilde{W}_A^{\text{ext}}(t)}{dt} \geq -\frac{d\Phi_A^{\text{neq}}(t)}{dt}. \quad (\text{B4})$$

This inequality is an extension of the principle of minimum work to a non-equilibrium regime.

Although we have derived Eqs. (B3) and (B4) for the specific equilibrium state 2, actually the value $(\Phi_A^{\text{neq}})_A$ is the same for any quasi-equilibrium state along $\beta^{\text{qst}}(t)$ and $x^{\text{qst}}(t)$. To illustrate this, we introduce a third equilibrium state 3 and consider the transition $A \rightarrow 3$ (see Fig. 8). Because $(\tilde{W}_A^{\text{ext}})_{A \rightarrow 2}^{\min} + (\tilde{W}_A^{\text{ext}})_{2 \rightarrow 3}^{\text{qst}} \geq (\tilde{W}_A^{\text{ext}})_{A \rightarrow 3}^{\min}$ for $A \rightarrow 2 \rightarrow 3$ and $(\tilde{W}_A^{\text{ext}})_{A \rightarrow 3}^{\min} + (\tilde{W}_A^{\text{ext}})_{3 \rightarrow 2}^{\text{qst}} \geq (\tilde{W}_A^{\text{ext}})_{A \rightarrow 2}^{\min}$ for $A \rightarrow 2 \rightarrow 3$, we have

$$(\tilde{W}_A^{\text{ext}})_{A \rightarrow 2}^{\min} + (\Phi_A^{\text{neq}})_2 = (\tilde{W}_A^{\text{ext}})_{A \rightarrow 3}^{\min} + (\Phi_A^{\text{neq}})_3, \quad (\text{B5})$$

where we have used $(\tilde{W}_A^{\text{ext}})_{2 \rightarrow 3}^{\text{qst}} = (\Phi_A^{\text{qst}})_3 - (\Phi_A^{\text{qst}})_2$. From Eq. (B1), this indicates that the non-equilibrium Massieu potential is independent of the choice of the equilibrium state 2.

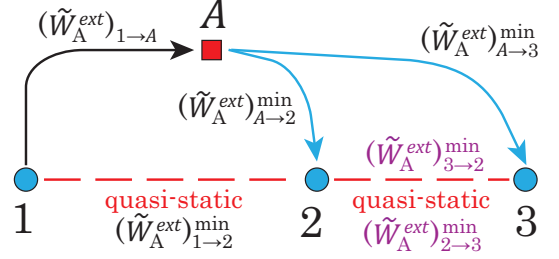


FIG. 8. Schematic showing that the non-equilibrium Massieu potential can be evaluated from any equilibrium state 3 instead of 2. To illustrate this, we consider the non-equilibrium-to-equilibrium path $A \rightarrow 3$, where we have introduced a third equilibrium state denoted by 3 (blue circle). The work between the two equilibrium states is denoted by $(\tilde{W}_A^{\text{ext}})_{2 \rightarrow 3}^{\text{qst}}$ and $(\tilde{W}_A^{\text{ext}})_{3 \rightarrow 2}^{\text{qst}}$, respectively.

Because the other potentials are interrelated through TDL transformations, we have

$$\frac{d\tilde{W}_A^{\text{int}}(t)}{dt} \geq -\frac{d\Xi_A^{\text{neq}}(t)}{dt}, \quad (\text{B6})$$

$$\frac{d\tilde{Q}_A^{\text{ext}}(t)}{dt} \leq \frac{d\Lambda_A^{\text{neq}}(t)}{dt}, \quad (\text{B7})$$

and

$$\frac{d\tilde{Q}_A^{\text{int}}(t)}{dt} \leq \frac{d\Gamma_A^{\text{neq}}(t)}{dt}. \quad (\text{B8})$$

For an isothermal case, from the definitions $F_A^{\text{neq}}(t) = -\Phi_A^{\text{neq}}(t)/\beta$ and $G_A^{\text{neq}}(t) = -\Xi_A^{\text{neq}}(t)/\beta$, we have

$$\frac{dW_A^{\text{ext}}(t)}{dt} \geq \frac{dF_A^{\text{neq}}(t)}{dt} \quad (\text{B9})$$

and

$$\frac{dW_A^{\text{int}}(t)}{dt} \geq \frac{dG_A^{\text{neq}}(t)}{dt}. \quad (\text{B10})$$

However, unlike in the Massieu-Planck case, the equality in Eqs. (B9) and (B10) cannot be obtained in general because the minimum DL work path in Fig. 6 is evaluated by optimizing both $\beta(t)$ and $x(t)$, while β has been fixed to introduce the Helmholtz energy as $F_A^{\text{neq}}(t) = -\Phi_A^{\text{neq}}(t)/\beta$.

The above discussion indicates that by including the thermostatic process, we may develop an efficient heat engine under non-equilibrium conditions.

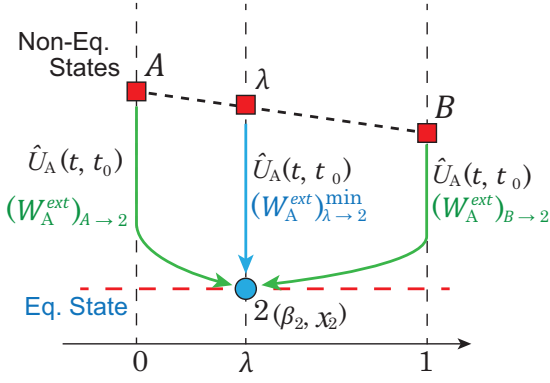


FIG. 9. Schematic for deriving convexity relations. The red squares represent the non-equilibrium states. The arrows are the relaxation paths to equilibrium state 2 described by the time-evolution operator $\hat{U}_A(t, t_0)$: The blue arrow is the DL minimum work path from state λ .

Appendix C: Convexity of non-equilibrium thermodynamic potentials as functions of extensive variables

To obtain stable thermodynamic properties, the thermodynamic potential must be a convex function of the work variables. Even in the non-equilibrium case, we find that convexity holds under certain conditions. Here, we show this in the case of the SB model. Because other potentials can be discussed similarly, we limit our discussion here to the case of a non-equilibrium Massieu potential.

We consider three non-equilibrium states A , B , and λ ($\lambda \in [0, 1]$) with the same initial inverse temperature $\beta(t_0)$ at time t_0 . We then assume that the state λ satisfies the relation

$$(W_A)_\lambda = (1 - \lambda)(W_A)_A + \lambda(W_A)_B, \quad (C1)$$

where $(W_A)_A = (W_A(p, q; t))_A$ and $(W_A)_B = (W_A(p, q; t))_B$ are Wigner distributions in the quantum case (or phase space distributions in the classical case) in the A and B states. The time-evolution operator for a subsystem is expressed as $\hat{U}_A(t, t_0) = \exp[-\int \hat{\mathcal{L}}(p, q) dt]$, where $\hat{\mathcal{L}}(p, q)$ is the Liouville operator, which includes fluctuation and dissipation operators for equilibration. In the quantum case, $\hat{\mathcal{L}}(p, q)$ acts on W_A , which is represented by hierarchical elements.^{30,31,52} We then obtain the relations for the extensive variable and internal energies as

$$(X_A)_\lambda(t) = (1 - \lambda)(X_A)_A(t) + \lambda(X_A)_B(t) \quad (C2)$$

and

$$(U_A)_\lambda(t) = (1 - \lambda)(U_A)_A(t) + \lambda(U_A)_B(t), \quad (C3)$$

where we have defined $(X_A)_\alpha(t) = \text{tr}_{\text{tot}}\{X_A(q)\hat{U}_{\text{tot}}(t, t_0)(W_{\text{tot}})_\alpha\}$ and $(U_A)_\alpha(t) =$

$\text{tr}_{\text{tot}}\{[p^2/2m + U(q)]\hat{U}_{\text{tot}}(t, t_0)(W_{\text{tot}})_\alpha\}$ for $\alpha = A, B$, and λ . Thus, from Eq. (2), the DL extensive work $(W_A^{ext})_\alpha(t, t_0)$ ($\alpha = A, B$, and λ), performed between times t_0 and t also satisfies the equality

$$(W_A^{ext})_\lambda(t, t_0) = (1 - \lambda)(W_A^{ext})_A(t, t_0) + \lambda(W_A^{ext})_B(t, t_0) \quad (C4)$$

The DL minimum work path from the state λ to the equilibrium state 2 is described by $\hat{U}_A(t, t_0)$ (see Fig. 9). This indicates that when t is large, the intensive variables must be $\beta(t) \rightarrow \beta_2$ and $x(t) \rightarrow x_2$, where β_2 and x_2 are the values at the equilibrium state 2. Therefore, the processes starting from A and B also relax to the equilibrium state 2 as $t \rightarrow \infty$. Then, from Eq. (C4), we obtain

$$(W_A^{ext})_{\lambda \rightarrow 2}^{\min} = (1 - \lambda)(W_A^{ext})_{A \rightarrow 2} + \lambda(W_A^{ext})_{B \rightarrow 2}. \quad (C5)$$

Using the inequality $(W_A^{ext})_{\alpha \rightarrow 2} \geq (W_A^{ext})_{\lambda \rightarrow 2}^{\min}$ for the states $\alpha = A$ and B , and Eq. (B1), we obtain the inequality to prove convexity as

$$(1 - \lambda)(\Phi_A^{\text{neq}})_A + \lambda(\Phi_A^{\text{neq}})_B \leq (\Phi_A^{\text{neq}})_\lambda, \quad (C6)$$

where $(\Phi_A^{\text{neq}})_\alpha$ is the non-equilibrium Massieu potential in the state α ($\alpha = A, B$, and λ). When A and B are in equilibrium states, we obtain the convexity relation in the quasi-static case for fixed inverse temperature using the inequality for the Massieu potential in Table VIII as⁵¹

$$(1 - \lambda)(\Phi_A^{\text{qst}})_A + \lambda(\Phi_A^{\text{qst}})_B \leq (\Phi_A^{\text{qst}})_\lambda. \quad (C7)$$

We summarize the convexity and concavity properties for the other non-equilibrium thermodynamic potential in Table VII.

Appendix D: Inequality between non-equilibrium and quasi-static thermodynamic potentials

Under given conditions, the non-equilibrium DL thermodynamic potentials are smaller than the quasi-static ones. Here, we derive the inequalities between the quasi-static and non-equilibrium thermodynamic potentials.

We consider a non-equilibrium-to-equilibrium transition $A \rightarrow 2$ from time t_1 to t_2 described by the inverse temperature $\beta(t)$ and the extensive variable $X_A^{\text{neq}}(t)$. The DL extensive work in this process is evaluated as

$$\begin{aligned} \int_{t_1}^{t_2} \left[U_A(t') \frac{d\beta(t')}{dt'} - \tilde{x}(t') \frac{dX_A^{\text{neq}}(t')}{dt'} \right] dt' \\ = \tilde{x}_2 (X_A^{\text{neq}}(t_2) - X_A^{\text{neq}}(t_1)), \end{aligned} \quad (D1)$$

where we have assumed that $\beta(t_1) = \beta_2$ and $X_A^{\text{neq}}(t_1) = (X_A^{\text{qst}})_2$, and that $\beta_2 = \beta(t)$ and $\tilde{x}_2 = \tilde{x}(t)$ for time $t > t_1$, to make the subsystem relax to the equilibrium state 2 at time t_2 . Because $X_A^{\text{neq}}(t_2) = (X_A^{\text{qst}})_2 = X_A^{\text{neq}}(t_1)$, the right-hand side of Eq. (D1) vanishes. Thus, the net DL

TABLE VII. Inequalities holding between the non-equilibrium state at time t_1 and the equilibrium state at time t_2 , together with the conditions under which these inequalities hold. From these inequalities, we find that, for example, for a given inverse temperature and electric field, the non-equilibrium Planck potential takes its maximum value when the state is in equilibrium.

| neq Potentials | Convexity and Concavity | Condition |
|----------------|--|---|
| Massieu | $(1 - \lambda)(\Phi_A^{\text{neq}})_A + \lambda(\Phi_A^{\text{neq}})_B \leq (\Phi_A^{\text{neq}})_\lambda$ | $\beta_A = \beta_B = \beta_\lambda$ |
| Planck | $(1 - \lambda)(\Xi_A^{\text{neq}})_A + \lambda(\Xi_A^{\text{neq}})_B \leq (\Xi_A^{\text{neq}})_\lambda$ | $\beta_A = \beta_B = \beta_\lambda$ and $\tilde{x}_A = \tilde{x}_B = \tilde{x}_\lambda$ |
| Helmholtz | $(1 - \lambda)(F_A^{\text{neq}})_A + \lambda(F_A^{\text{neq}})_B \geq (F_A^{\text{neq}})_\lambda$ | $\beta_A = \beta_B = \beta_\lambda$ |
| Gibbs | $(1 - \lambda)(G_A^{\text{neq}})_A + \lambda(G_A^{\text{neq}})_B \geq (G_A^{\text{neq}})_\lambda$ | $\beta_A = \beta_B = \beta_\lambda$ and $x_A = x_B = x_\lambda$ |

TABLE VIII. Inequalities for Massieu–Planck potentials holding between the non-equilibrium state A at time t_1 and the equilibrium state 2 at time t_2 , together with the conditions under which these inequalities hold. From these inequalities, we find that, for example, for a given inverse temperature and intensive variable, the non-equilibrium Planck potential takes its maximum value when A is in the equilibrium state.

| neq Potentials | Inequalities | Condition |
|----------------|--|---|
| Massieu | $\Phi_A^{\text{qst}}(t_2) \geq \Phi_A^{\text{neq}}(t_1)$ | $\beta(t_1) = \beta(t_2)$ and $X_A(t_1) = X_A(t_2)$ |
| Planck | $\Xi_A^{\text{qst}}(t_2) \geq \Xi_A^{\text{neq}}(t_1)$ | $\beta(t_1) = \beta(t_2)$ and $\tilde{x}(t_1) = \tilde{x}(t_2)$ |
| C–Entropy | $\Lambda_A^{\text{qst}}(t_2) \geq \Lambda_A^{\text{neq}}(t_1)$ | $U_A(t_1) = U_A(t_2)$ and $X_A(t_1) = X_A(t_2)$ |
| B–Entropy | $\Gamma_A^{\text{qst}}(t_2) \geq \Gamma_A^{\text{neq}}(t_1)$ | $U_A(t_1) = U_A(t_2)$ and $\tilde{x}(t_1) = \tilde{x}(t_2)$ |

TABLE IX. Inequalities for Helmholtz–Gibbs potentials holding between the non-equilibrium state at time t_1 and the equilibrium state at time t_2 , together with the conditions under which these inequalities hold.

| neq Potentials | Inequalities | Condition |
|-----------------|--|---|
| Helmholtz | $F_A^{\text{qst}}(t_2) \leq F_A^{\text{neq}}(t_1)$ | $T(t_1) = T(t_2)$ and $X_A(t_1) = X_A(t_2)$ |
| Gibbs | $G_A^{\text{qst}}(t_2) \leq G_A^{\text{neq}}(t_1)$ | $T(t_1) = T(t_2)$ and $x(t_1) = x(t_2)$ |
| Internal Energy | $U_A(t_2) \leq U_A(t_1)$ | $S_A^{\text{neq}}(t_1) = S_A^{\text{qst}}(t_2)$ and $X_A(t_1) = X_A(t_2)$ |
| Enthalpy | $H_A(t_2) \leq H_A(t_1)$ | $S_A^{\text{neq}}(t_1) = S_A^{\text{qst}}(t_2)$ and $x(t_1) = x(t_2)$ |

extensive work is zero, and so the DL minimum work principle reduces to $0 \geq (\Phi_A^{\text{neq}})_{A \rightarrow 2}$, from which it follows that $\Phi_A^{\text{qst}}(t_2) \geq \Phi_A^{\text{neq}}(t_1)$.

The inequalities for the other DL thermodynamic potentials are obtained in the same manner. We summarize the results in Tables VIII and IX.

In Fig. 10, to illustrate the inequalities presented in Table VIII, we plot the difference between the quasi-static and non-equilibrium Planck potential, $\Delta\Xi_A(t) = \Xi_A^{\text{qst}}[\beta(t), \tilde{x}(t)] - \Xi_A^{\text{neq}}(t)$, for one cycle of the Stirling engine described in Sec. III D. As can be seen, $\Delta\Xi_A(t)$ is always positive and satisfies the inequalities in Table VIII.

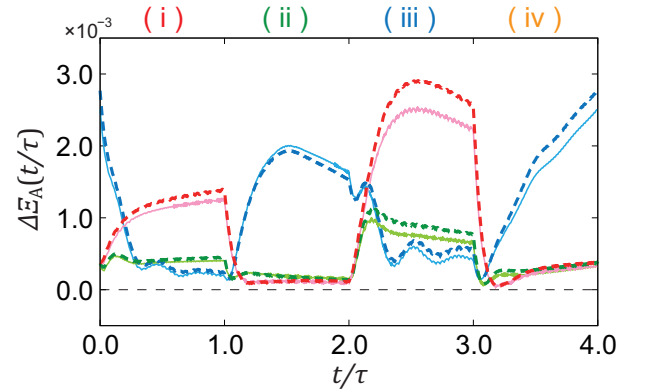


FIG. 10. Difference between the quasi-static and non-equilibrium Planck potential in the quantum and classical cases (solid and dashed curves, respectively) for one cycle of the Stirling engine. The blue, green, and red curves represent the cases of weak ($A = 0.5$), intermediate ($A = 1.0$), and strong ($A = 1.5$) SB coupling, respectively.

¹S. Carnot, *Reflexions sur la puissance motrice du feu* (Chez Bachelier Libraire, Quai des Augustins, Paris, 1824).

²H. T. Quan, Y. D. Wang, Y.-x. Liu, C. P. Sun, and F. Nori, “Maxwell’s demon assisted thermodynamic cycle in superconducting quantum circuits,” *Phys. Rev. Lett.* **97**, 180402 (2006).

³M. Esposito, U. Harbola, and S. Mukamel, “Nonequilibrium fluctuations, fluctuation theorems, and counting statistics in quantum systems,” *Rev. Mod. Phys.* **81**, 1665–1702 (2009).

⁴M. Campisi, P. Hänggi, and P. Talkner, “Colloquium: Quantum fluctuation relations: Foundations and applications,” *Rev. Mod. Phys.* **83**, 771–791 (2011).

⁵R. Kosloff and A. Levy, “Quantum heat engines and refrigerators: Continuous devices,” *Annual Review of Physical Chemistry* **65**, 365–393 (2014), PMID: 24689798.

⁶M. Esposito, M. A. Ochoa, and M. Galperin, “Na-

ture of heat in strongly coupled open quantum systems,” *Phys. Rev. B* **92**, 235440 (2015).

⁷R. Schmidt, M. F. Carusela, J. P. Pekola, S. Suomela, and J. Ankerhold, “Work and heat for two-level systems in dissipative environments: Strong driving and non-Markovian dynamics,” *Phys. Rev. B* **91**, 224303 (2015).

- ⁸R. Uzdin, A. Levy, and R. Kosloff, “Equivalence of quantum heat machines, and quantum-thermodynamic signatures,” *Phys. Rev. X* **5**, 031044 (2015).
- ⁹R. S. Whitney, “Non-Markovian quantum thermodynamics: Laws and fluctuation theorems,” *Phys. Rev. B* **98**, 085415 (2018).
- ¹⁰H. T. Quan, Y.-x. Liu, C. P. Sun, and F. Nori, “Quantum thermodynamic cycles and quantum heat engines,” *Phys. Rev. E* **76**, 031105 (2007).
- ¹¹K. Maruyama, F. Nori, and V. Vedral, “Colloquium: The physics of maxwell’s demon and information,” *Rev. Mod. Phys.* **81**, 1–23 (2009).
- ¹²K. Ono, S. N. Shevchenko, T. Mori, S. Moriyama, and F. Nori, “Analog of a quantum heat engine using a single-spin qubit,” *Phys. Rev. Lett.* **125**, 166802 (2020).
- ¹³P. Talkner and P. Hänggi, “Colloquium: Statistical mechanics and thermodynamics at strong coupling: Quantum and classical,” *Rev. Mod. Phys.* **92**, 041002 (2020).
- ¹⁴L. M. Cangemi, V. Cataudella, G. Benenti, M. Sasseti, and G. De Filippis, “Violation of thermodynamics uncertainty relations in a periodically driven work-to-work converter from weak to strong dissipation,” *Phys. Rev. B* **102**, 165418 (2020).
- ¹⁵P. Strasberg and A. Winter, “First and second law of quantum thermodynamics: A consistent derivation based on a microscopic definition of entropy,” *PRX Quantum* **2**, 030202 (2021).
- ¹⁶C. Cockrell and I. J. Ford, “Stochastic thermodynamics in a non-markovian dynamical system,” *Phys. Rev. E* **105**, 064124 (2022).
- ¹⁷P. Talkner and P. Hänggi, “Colloquium: Statistical mechanics and thermodynamics at strong coupling: Quantum and classical,” *Rev. Mod. Phys.* **92**, 041002 (2020).
- ¹⁸R. Dann and R. Kosloff, “Unification of the first law of quantum thermodynamics,” *New Journal of Physics* **25**, 043019 (2023).
- ¹⁹A. Ferreri, V. Macri, F. K. Wilhelm, F. Nori, and D. E. Bruschi, “Quantum field heat engine powered by phonon-photon interactions,” *Phys. Rev. Res.* **5**, 043274 (2023).
- ²⁰S. Sakamoto and Y. Tanimura, “Open quantum dynamics theory for non-equilibrium work: Hierarchical equations of motion approach,” *Journal of the Physical Society of Japan* **90**, 033001 (2021).
- ²¹A. Kato and Y. Tanimura, “Quantum heat transport of a two-qubit system: Interplay between system-bath coherence and qubit-qubit coherence,” *The Journal of Chemical Physics* **143**, 064107 (2015).
- ²²A. Kato and Y. Tanimura, “Quantum heat current under non-perturbative and non-Markovian conditions: Applications to heat machines,” *The Journal of Chemical Physics* **145**, 224105 (2016).
- ²³A. J. Leggett, S. Chakravarty, A. T. Dorsey, M. P. A. Fisher, A. Garg, and W. Zwerger, “Dynamics of the dissipative two-state system,” *Rev. Mod. Phys.* **59**, 1–85 (1987).
- ²⁴A. Caldeira and A. Leggett, “Path integral approach to quantum brownian motion,” *Physica A: Statistical Mechanics and its Applications* **121**, 587–616 (1983).
- ²⁵H. Grabert, P. Schramm, and G.-L. Ingold, “Quantum brownian motion: The functional integral approach,” *Physics Reports* **168**, 115–207 (1988).
- ²⁶U. Weiss, *Quantum Dissipative Systems*, 4th ed. (WORLD SCIENTIFIC, 2012).
- ²⁷Y. Tanimura and R. Kubo, “Time evolution of a quantum system in contact with a nearly Gaussian-Markoffian noise bath,” *Journal of the Physical Society of Japan* **58**, 101–114 (1989).
- ²⁸Y. Tanimura, “Nonperturbative expansion method for a quantum system coupled to a harmonic-oscillator bath,” *Phys. Rev. A* **41**, 6676–6687 (1990).
- ²⁹Y. Tanimura, “Reduced hierarchical equations of motion in real and imaginary time: Correlated initial states and thermodynamic quantities,” *The Journal of Chemical Physics* **141**, 044114 (2014).
- ³⁰Y. Tanimura, “Stochastic Liouville, Langevin, Fokker-Planck, and master equation approaches to quantum dissipative systems,” *Journal of the Physical Society of Japan* **75**, 082001 (2006).
- ³¹Y. Tanimura, “Numerically ”exact” approach to open quantum dynamics: The hierarchical equations of motion (HEOM),” *The Journal of Chemical Physics* **153**, 020901 (2020).
- ³²Y. Tanimura, “Real-time and imaginary-time quantum hierarchal Fokker-Planck equations,” *The Journal of Chemical Physics* **142**, 144110 (2015).
- ³³A. Ishizaki and Y. Tanimura, “Quantum dynamics of system strongly coupled to low-temperature colored noise bath: Reduced hierarchy equations approach,” *Journal of the Physical Society of Japan* **74**, 3131–3134 (2005).
- ³⁴N. Makri, “Numerical path integral techniques for long time dynamics of quantum dissipative systems,” *Journal of Mathematical Physics* **36**, 2430–2457 (1995).
- ³⁵N. Makri and D. E. Makarov, “Tensor propagator for iterative quantum time evolution of reduced density matrices. I. Theory,” *The Journal of Chemical Physics* **102**, 4600–4610 (1995).
- ³⁶N. Makri and D. E. Makarov, “Tensor propagator for iterative quantum time evolution of reduced density matrices. II. Numerical methodology,” *The Journal of Chemical Physics* **102**, 4611–4618 (1995).
- ³⁷M. Thorwart, P. Reimann, and P. Hänggi, “Iterative algorithm versus analytic solutions of the parametrically driven dissipative quantum harmonic oscillator,” *Phys. Rev. E* **62**, 5808–5817 (2000).
- ³⁸V. Jadhao and N. Makri, “Iterative monte carlo for quantum dynamics,” *The Journal of Chemical Physics* **129**, 161102 (2008).
- ³⁹N. Makri, “Blip decomposition of the path integral: Exponential acceleration of real-time calculations on quantum dissipative systems,” *The Journal of Chemical Physics* **141**, 134117 (2014).
- ⁴⁰D. Segal, A. J. Millis, and D. R. Reichman, “Numerically exact path-integral simulation of nonequilibrium quantum transport and dissipation,” *Phys. Rev. B* **82**, 205323 (2010).
- ⁴¹H.-D. Meyer, U. Manthe, and L. Cederbaum, “The multi-configurational time-dependent hartree approach,” *Chemical Physics Letters* **165**, 73–78 (1990).
- ⁴²U. Manthe, H. Meyer, and L. S. Cederbaum, “Wavepacket dynamics within the multiconfiguration Hartree framework: General aspects and application to NOCl,” *The Journal of Chemical Physics* **97**, 3199–3213 (1992).
- ⁴³H. Wang and M. Thoss, “Quantum dynamical simulation of electron-transfer reactions in an anharmonic environment,” *The Journal of Physical Chemistry A* **111**, 10369–10375 (2007).
- ⁴⁴S. Sakamoto and Y. Tanimura, “Numerically ”exact” simulations of entropy production in the fully quantum regime: Boltzmann entropy vs von Neumann entropy,” *The Journal of Chemical Physics* **153**, 234107 (2020).
- ⁴⁵L. Song and Q. Shi, “Hierarchical equations of motion method applied to nonequilibrium heat transport in model molecular junctions: Transient heat current and high-order moments of the current operator,” *Phys. Rev. B* **95**, 064308 (2017).
- ⁴⁶H. J. Gong, Y. Wang, X. Zheng, R. Xu, and Y. Yan, “Nonequilibrium work distributions in quantum impurity system-bath mixing processes,” *The Journal of Chemical Physics* **157**, 054109 (2022).
- ⁴⁷C. L. Latune, G. Pleasance, and F. Petruccione, “Cyclic quantum engines enhanced by strong bath coupling,” *Phys. Rev. Appl.* **20**, 024038 (2023).
- ⁴⁸V. Boettcher, R. Hartmann, K. Beyer, and W. T. Strunz, “Dynamics of a strongly coupled quantum heat engine—Computing bath observables from the hierarchy of pure states,” *The Journal of Chemical Physics* **160**, 094108 (2024).
- ⁴⁹S. Koyanagi and Y. Tanimura, “The laws of thermodynamics for quantum dissipative systems: A quasi-equilibrium Helmholtz energy approach,” *The Journal of Chemical Physics* **157**, 014104 (2022).
- ⁵⁰S. Koyanagi and Y. Tanimura, “Numerically ”exact” simulations of a quantum carnot cycle:

- Analysis using thermodynamic work diagrams,” *The Journal of Chemical Physics* **157**, 084110 (2022).
- ⁵¹S. Koyanagi and Y. Tanimura, “Classical and quantum thermodynamic theory described by a system–baths model: The dimensionless minimum work principle,” *The Journal of Chemical Physics* **xxx**, xxxxx (2024), [2405.16787](#).
- ⁵²T. Ikeda and Y. Tanimura, “Low-temperature quantum Fokker-Planck and Smoluchowski equations and their extension to multistate systems,” *Journal of Chemical Theory and Computation* **15**, 2517–2534 (2019).
- ⁵³Y. Oono, *Perspectives on Statistical Thermodynamics* (Cambridge University Press, 2017).
- ⁵⁴F. Massieu, “Sur les fonctions caractéristiques des divers fluides,” *CR Acad. Sci. Paris* **69**, 858–862 (1869).
- ⁵⁵M. Planck, *Vorlesungen über Thermodynamik* (De Gruyter, 1922).
- ⁵⁶E. A. Guggenheim, *Thermodynamics: An Advanced Treatment for Chemists and Physicists* (North Holland, 1986).
- ⁵⁷Z. Rant, “Exergie, ein neues wort für ’technische arbeitsfähigkeit,’” (1956) p. 33.
- ⁵⁸M. A. Rosen and I. Dincer, “Exergy as the confluence of energy, environment and sustainable development,” *Exergy, An International Journal* **1**, 3–13 (2001).
- ⁵⁹P. Ullersma, “An exactly solvable model for brownian motion: I. derivation of the langevin equation,” *Physica* **32**, 27–55 (1966).
- ⁶⁰P. Ullersma, “An exactly solvable model for brownian motion: II. derivation of the fokker-planck equation and the master equation,” *Physica* **32**, 56–73 (1966).
- ⁶¹Y. Tanimura and P. G. Wolynes, “Quantum and classical Fokker-Planck equations for a Gaussian-Markovian noise bath,” *Phys. Rev. A* **43**, 4131–4142 (1991).
- ⁶²Y. Tanimura and P. G. Wolynes, “The interplay of tunneling, resonance, and dissipation in quantum barrier crossing: A numerical study,” *The Journal of Chemical Physics* **96**, 8485–8496 (1992).
- ⁶³A. Kato and Y. Tanimura, “Quantum suppression of ratchet rectification in a Brownian system driven by a biharmonic force,” *The Journal of Physical Chemistry B* **117**, 13132–13144 (2013).
- ⁶⁴S. Koyanagi and Y. Tanimura, “Thermodynamic hierarchical equations of motion in phase space representation,” (2024), [xxxxxx:xxxxxx](#).